

UNIVERSIDADE DE LISBOA  
FACULDADE DE CIÊNCIAS  
DEPARTAMENTO DE FÍSICA



**Ciências**  
**ULisboa**

**Generation of hiPSC-derived motor neurons in  
compartmentalization devices for the development of a  
polarized neuronal model in vitro**

Ana Beatriz Figueiredo da Cunha Machado

**Mestrado em Engenharia Biomédica e Biofísica**

Dissertação orientada por:  
Daniela Maria Rossi  
Sofia Rita Cardoso Fernandes



## **Acknowledgments**

I would like to express my gratitude to all those who have supported me during these five years of university and in my journey to complete this thesis.

In the first place, I would like to thank Dra. Daniela Rossi, my supervisor in the laboratory, for the opportunity to carry out my work in her laboratory and for her guidance and support, which were fundamental to the success of this thesis.

I would also like to express my gratitude to Dra. Liliana and Dra. Chiara, whose knowledge and expertise greatly enhanced my experience. I am thankful for the opportunity to have worked with you.

Furthermore, I would like to thank Dra. Sofia Fernandes, my supervisor at the university, for the opportunity to work on this project and for her academic guidance and feedback during this time.

I am profoundly thankful to my family, especially my parents, my endless source of strength, for their unconditional love and support. None of this would have been possible without them. I would also like to thank my godfather and my aunt for their support and love during challenging times.

I cannot go without thanking my Italian friends: Valentina, Massi, Ludovica, and Paola. Thank you for welcoming me so well and for your kindness. Your friendship means the world to me. I couldn't have done any of this without you.

I would like to extend my gratitude to my friends Maria and Beatriz, who have accompanied me throughout these five years of university and during my thesis. These years wouldn't have been the same without you. I am forever grateful to have you in my life.

Lastly, I would like to thank my friend Joana, my dear friend from school, who has always been there for me through all this time.

## Abstract

Amyotrophic Lateral Sclerosis (ALS) is the most prevalent form of Motor Neuron Diseases (MNDs), representing a progressive neurodegenerative condition that affects nerve cells in the motor cortex and spinal cord. ALS manifests as a combination of upper and lower motor neuron deficits, profoundly affecting both limb and bulbar muscles. This study explored the potential of the differentiation of Induced Pluripotent Stem Cells (iPSCs) into Motor Neurons (MNs) to create an *in vitro* model that mimics the disease's characteristics.

In order to do this, three different lines of iPSC-derived cells from ALS patients were used, as well as a control line from a healthy individual. A documented differentiation protocol was applied, followed by immunocytochemical and morphological analysis and gene expression studies. These procedures aimed at evaluating both the features of the generated MNs and the efficiency of the differentiation protocol.

According to the results, all iPSC lines have successfully differentiated into MNs, with a noticeable variability in differentiation efficiency and neurite length between ALS and control cell lines. Furthermore, unique ALS-linked phenotypes were revealed by the differential expression of stage-specific markers.

In conclusion, this study supports the use of iPSCs as a powerful tool in ALS disease modeling. It provides a better understanding of ALS pathogenesis at the cellular level, and, through the investigation of the genetic and phenotypic variability of the disease, iPSC models allow for the development of personalized treatments and drug screening tools, offering more effective treatments in ALS.

**Keywords: Amyotrophic Lateral Sclerosis (ALS), Induced Pluripotent Stem Cells (iPSCs), Motor Neuron Disease (MND), Motor Neuron Differentiation, Disease Modeling.**

## Resumo

As doenças neurodegenerativas, como a doença de Alzheimer, Parkinson e Esclerose Lateral Amiotrófica (ELA) são doenças caracterizadas pela degeneração progressiva de células neuronais. A ELA é uma doença neurodegenerativa caracterizada pela perda progressiva de neurónios motores no cérebro, tronco cerebral e medula espinhal. A sintomatologia destes pacientes geralmente inclui fraqueza e atrofia muscular, com eventual paralisia, resultando em morte entre 3 a 5 anos depois do diagnóstico, normalmente devido a falência respiratória. A ELA pode ser classificada em duas principais categorias: ELA familiar, associada a um histórico familiar conhecido da doença, responsável por cerca de 10% dos casos; e a ELA esporádica, sem histórico familiar conhecido, o qual corresponde aos restantes 90% dos casos. Importa referir também que, do ponto de vista clínico, a ELA familiar e a ELA esporádica apresentam os mesmos sintomas, sendo por isso indistinguíveis. A ELA é uma doença neurodegenerativa complexa com uma componente genética. Ao longo dos anos, foram identificados vários genes associados à ELA, sendo os mais frequentes: *Superoxide dismutase 1 (SOD1)*, *Fused in sarcoma (FUS)*, *TAR DNA-binding protein 43 (TDP-43 ou TARDBP)* e *Chromosome 9 open reading frame 72 (C9ORF72)*.

Nos últimos anos, os avanços na tecnologia de células estaminais têm proporcionado inúmeras possibilidades para estudos sobre a ELA. Deste modo, surgiram as células estaminais pluripotentes induzidas (iPSCs). As iPSCs são derivadas de células somáticas<sup>1</sup> que foram reprogramadas a um estado pluripotente, semelhante ao das células estaminais embrionárias. Estas células surgiram como uma ferramenta para o estudo de diversas doenças em ambiente controlado, possibilitando a diferenciação de diversos tipos celulares específicos. No contexto da ELA, as iPSCs permitem a criação de modelos *in vitro* da doença, proporcionando uma maior compreensão das mudanças celulares e moleculares a esta associadas. Estes modelos são cruciais para o estudo da progressão da doença e para a possível identificação de novos alvos terapêuticos.

Deste modo, este estudo incidiu sobre a diferenciação de iPSCs em neurónios motores de pacientes com ELA. Assim, foram utilizadas três linhas celulares derivadas de iPSCs de pacientes com ELA: uma de sALS e duas de fALS (com mutações nos genes *C9ORF72* e *SOD1*). Para além disso, foi utilizada uma linha celular de controlo, derivada de iPSCs de um indivíduo saudável. O processo de diferenciação seguiu um protocolo documentado na literatura e adotado pelo laboratório onde este estudo foi desenvolvido com algumas modificações. Este protocolo incluía uma fase de indução neural, seguida de uma fase de maturação dos neurónios motores.

Para avaliar o sucesso do processo de diferenciação e as características dos neurónios motores obtidos, realizaram-se testes de imunocitoquímica para detetar a presença de marcadores específicos em cada fase do processo. Adicionalmente, procedeu-se à quantificação do comprimento dos neuritos<sup>2</sup> e à avaliação da expressão génica destes marcadores utilizando a técnica de Transcrição Reversa seguida de Reação em Cadeia da Polimerase (RT-PCR) seguida de eletroforese. Estas técnicas permitem uma maior compreensão das diferenças morfológicas e funcionais entre as diferentes linhas celulares.

---

<sup>1</sup> Células somáticas: Uma célula somática refere-se a uma célula não reprodutiva de um organismo multicelular, distinguindo-a das células germinativas. As células somáticas compõem a maior parte dos tecidos e órgãos do corpo e não participam da reprodução.

<sup>2</sup> Neurito: Qualquer projeção a partir do corpo celular de um neurónio. Termo geralmente utilizado para referir axónios e dendrites de neurónios imaturos ou em desenvolvimento [1]

Os resultados demonstram que as iPSCs de todas as linhas celulares se diferenciaram com sucesso em neurónios motores, com uma variabilidade significativa na eficiência de diferenciação e no comprimento dos neuritos. Para além disso, a comparação destes resultados com a expressão diferencial de marcadores neuronais específicos permitiu estabelecer correlações entre as diferentes mutações e a linha de controlo. O uso das iPSCs não só permite uma compreensão detalhada dos fenótipos celulares, como também acarreta vantagens relativamente aos modelos animais. Porém, apesar destes modelos terem permitido o alargamento do conhecimento sobre os mecanismos da ELA, não permitem replicar totalmente a variabilidade genética e fenotípica verificada no ser humano.

Através da análise de resultados, é possível observar uma menor expressão do fator de transcrição HB9 na linha celular com a mutação no gene *SOD1*, o que pode estar associado às características intrínsecas desta mutação. Como o HB9 está envolvido na manutenção da identidade e sobrevivência dos neurónios motores, a sua baixa expressão em pacientes com esta mutação pode refletir uma disfunção dos neurónios motores, progressão da doença, regeneração comprometida ou uma desregulação da expressão génica.

Além disso, a análise do comprimento dos neuritos mostrou que os neurónios motores derivados de iPSCs de pacientes com ELA apresentam um menor comprimento em comparação com os dos neurónios derivados da linha de controlo, à exceção dos neurónios da linha com mutação no gene *SOD1*. Este resultado é inesperado uma vez que esta linha apresenta a menor eficiência de diferenciação. Contudo, existem duas possíveis explicações. Em primeiro lugar, apesar da taxa de eficiência ser mais baixa, pode ter ocorrido um maior crescimento dos neuritos dos neurónios motores que efetivamente se diferenciaram. Em segundo lugar, isto pode significar que existem mecanismos compensatórios ou características específicas da mutação *SOD1* que afetam a extensão dos neuritos. Esta característica fenotípica serve como um importante marcador de doença no contexto de culturas celulares.

Estes resultados demonstram que o uso de iPSCs derivadas de pacientes com ELA é uma ferramenta valiosa para estudar os mecanismos da doença e da sua progressão, bem como para o desenvolvimento de novos fármacos e de terapias personalizadas. A criação destes modelos celulares *in vitro* permite replicar as condições celulares específicas de pacientes com diferentes mutações associadas à ELA, permitindo por sua vez testar novas terapias de forma mais precisa, tendo em consideração a variabilidade genética e fenotípica associada às diferentes mutações. A capacidade de gerar iPSCs específicas de pacientes com ELA contribui para a criação de tratamentos personalizados que podem ser ajustados aos perfis genéticos individuais, aumentando a eficiência terapêutica e minimizando os efeitos adversos, contribuindo para uma melhor qualidade de vida destes pacientes.

Apesar deste estudo evidenciar a importância das iPSCs para o estudo da ELA, existem limitações associadas à sua utilização que devem ser levadas em consideração. O processo de reprogramação, embora eficiente, apresenta algumas limitações relacionadas com possíveis mudanças genéticas e epigenéticas induzidas pela reprogramação, contribuindo para a variabilidade genética entre linhas celulares. Para além disso, a longa duração dos protocolos de diferenciação associada à necessidade de protocolos altamente especializados para a manutenção destas células pode limitar a sua aplicação imediata em contexto clínico. No entanto, têm sido feitos vários esforços no sentido da padronização e otimização dos protocolos de diferenciação, de modo a diminuir e até eliminar estas limitações, tornando a aplicação das iPSCs em ambiente

clínico cada vez mais possível.

Em conclusão, este estudo realça a importância do uso das iPSCs no estudo da ELA e de outras doenças neurodegenerativas. O uso das iPSCs reveste-se da maior importância para alargar o conhecimento acerca dos mecanismos patológicos da ELA, servindo de base para o desenvolvimento de novas abordagens terapêuticas, incluindo o desenvolvimento de tratamentos personalizados e de novos fármacos. Para além disso, a combinação destes modelos de doença com tecnologias emergentes, como a edição genética, pode promover o desenvolvimento de novas terapias mais eficazes e personalizadas, com o objetivo de melhorar a qualidade de vida dos pacientes com ELA. Assim, é possível concluir que as iPSCs são uma ferramenta fundamental para o estudo da ELA. As iPSCs permitem o desenvolvimento de modelos de doença, os quais possibilitam uma maior compreensão dos seus mecanismos fisiopatológicos característicos, bem como criam novas oportunidades para a medicina de precisão, permitindo que cada tratamento seja adaptado às necessidades genéticas individuais de cada paciente. Todas estas aplicações representam oportunidades importantes para o tratamento e para a melhoria da qualidade de vida destes pacientes.

**Palavras-chave: Esclerose Lateral Amiotrófica (ELA), Células Estaminais Pluripotentes Induzidas (iPSCs), Doenças neurodegenerativas, Neurónios Motores.**

## Contents

<b>1</b>	<b>Motivation</b>	<b>1</b>
<b>2</b>	<b>Introduction</b>	<b>2</b>
2.1	Structure of the Nervous System.....	2
2.2	Neuron Structure .....	2
2.3	Motor Neuron.....	3
2.3.1	Upper MNs .....	3
2.3.2	Lower MNs.....	4
2.4	Amyotrophic Lateral Sclerosis (ALS) as a Motor Neuron Disease.....	6
2.4.1	Pathophysiology of ALS.....	7
2.4.2	Clinical Presentation.....	8
2.4.3	Genetic Basis of ALS .....	8
2.5	Stem Cells .....	11
2.6	Induced Pluripotent Stem Cells (iPSCs).....	16
2.6.1	Reprogramming Factors .....	17
2.6.2	Reprogramming Methods .....	19
2.6.3	Characterization of iPSCs.....	23
2.6.4	Neural Differentiation.....	24
2.6.5	Advantages of iPSCs compared to animal models .....	25
2.6.6	Limitations of iPSC .....	25
2.6.7	iPSCs Applications .....	26
2.6.8	iPSCs as a Disease Model and Drug Screening tool.....	27
2.6.9	iPSCs use in ALS.....	27
<b>3</b>	<b>Materials and Methods</b>	<b>29</b>
3.1	Induced Pluripotent Stem Cells: cell lines used and their maintenance .....	29
3.2	<i>Geltrex</i> Matrix .....	29
3.2.1	<i>Geltrex</i> Preparation.....	29
3.3	Detachment, splitting, and freezing procedures .....	30
3.4	Motor neuron differentiation protocol.....	31
3.5	Immunocytochemistry.....	35
3.5.1	Protocol.....	35
3.6	Quantification and Morphological analysis of $\beta$ TUB-Positive Motor Neurons.....	37
3.7	Analysis of ChAT expression levels .....	37
3.7.1	RNA extraction.....	37
3.7.2	Reverse-transcription and DNA synthesis .....	38
3.7.3	Reverse Transcription Polymerase Chain Reaction (RT-PCR) .....	39
3.7.4	Electrophoresis .....	40
3.8	Statistical Analysis .....	40

**4 Results and Discussion 41**

4.1 Generation and Evaluation of iPSC-derived ALS Motor Neurons.....41

4.2 Evaluation of the Differentiation Efficiency of iPSC-derived Motor Neurons .....49

4.3 Phenotypic Characterization of MNs Derived from iPSC: Neurite Length Evaluation .....51

4.4 Analysis of ChAT expression levels .....53

**5 Conclusion 54**

## List of Tables

2.1	Summary of the four most common ALS-associated genes [2], [3].....	11
2.2	Summary of the most important characteristics of ESCs, ASCs, and iPSCs.....	15
2.3	Summary of the Advantages and Disadvantages/Limitations of Integrating and Non-Integrating Methods. ....	22
3.1	Common constituents of all medium formulations.....	31
3.2	Medium A formulation.....	31
3.3	Medium B formulation.....	32
3.4	Medium C formulation.....	32
3.5	Medium D formulation.....	34
4.1	Differentiation Efficiency of iPSCs into MNs.....	50
4.2	Statistical Analysis of Differentiation Efficiency of iPSC-derived MNs.....	51
4.3	Average Neurite Length of iPSC-derived MNs.....	52
4.4	Statistical Analysis of Neurite Length of iPSC-derived MNs.....	52
A.1	Information about the different cell lines used.....	55
A.2	Immunocytochemistry on hiPSc in differentiation into MNs.....	56

## List of Figures

2.1	Schematic representation of a Nissl-stained motor neuron [4].	3
2.2	Schematic representation of the iPSC generation process [5].	24
3.1	a) Cell-counting chamber device; b) Chamber of a cell-counting chamber device.	33
3.2	1-key manual cell counter device.	34
3.3	Device used to place the coverslips during the immunocytochemistry experiment.	36
4.1	Schematic representation of the experimental timeline, indicating the respective markers to be identified in each phase.	42
4.2	Bright Field (BF) images of iPSC colonies from four different cell lines in maintenance culture: (A) 30HU-002 (NORM), (B) 30HU-004 (sALS), (C) CS52iALS-C9n6, and (D) Cs04iALS-SOD1H44Rn3. Scale bar = 200 $\mu$ m.	43
4.3	Bright Field (BF) images of iPSC colonies from four different cell lines in Medium A culture: 30HU-002 (NORM), (B) 30HU-004 (sALS), (C) CS52iALS-C9n6, and (D) Cs04iALS-SOD1H44Rn3. Scale bar = 100 $\mu$ m.	43
4.4	Immunocytochemical analysis of NEPs at DIV10, stained for the marker SOX1. The first row shows cells from the 30HU-002 (NORM) cell line, the second from the 30HU-004 (sALS) cell line, the third from the CS52iALS-C9n6 cell line, and the fourth from the 3Cs04iALS-SOD1H44Rn3 cell line. Scale bar = 50 $\mu$ m.	44
4.5	Bright Field (BF) images of iPSC colonies from four different cell lines in Medium B culture: 30HU-002 (NORM), (B) 30HU-004 (sALS), (C) CS52iALS-C9n6, and (D) Cs04iALS-SOD1H44Rn3. Scale bar = 100 $\mu$ m	45
4.6	Immunocytochemical analysis of MNPs at DIV17, stained for the marker OLIG2. The first row shows cells from the 30HU-002 (NORM) cell line, the second from the 30HU-004 (sALS) cell line, the third from the CS52iALS-C9n6 cell line, and the fourth from the Cs04iALS-SOD1H44Rn3 cell line. Scale bar = 50 $\mu$ m.	46
4.7	Bright Field (BF) images of iPSC colonies from four different cell lines in Medium C culture: 30HU-002 (NORM), (B) 30HU-004 (sALS), (C) CS52iALS-C9n6, and (D) Cs04iALS-SOD1H44Rn3, respectively. Scale bar = 200 $\mu$ m.	46
4.8	Immunocytochemical analysis of MNs at DIV30, stained for the marker HB9. The first row shows cells from the 30HU-002 (NORM) cell line, the second from the 30HU-004 (sALS) cell line, the third from the CS52iALS-C9n6 cell line, and the fourth from the Cs04iALS-SOD1H44Rn3 cell line. Scale bar = 50 $\mu$ m.	47
4.9	Immunocytochemical analysis of MNs at DIV30, stained for the markers ISL-1 and MAP2. The first row shows cells from the 30HU-002 (NORM) cell line, the second from the 30HU-004 (sALS) cell line, the third from the CS52iALS-C9n6 cell line, and the fourth from the Cs04iALS-SOD1H44Rn3 cell line. Scale bar = 50 $\mu$ m.	48
4.10	Bright Field (BF) images of iPSC colonies from four different cell lines in Medium D culture: 30HU-002 (NORM), (B) 30HU-004 (sALS), (C) CS52iALS-C9n6, and (D) Cs04iALS-SOD1H44Rn3, respectively. Scale bar = 50 $\mu$ m.	48
4.11	Immunocytochemical analysis of MNs at DIV40, stained for the markers ChAT and $\beta$ TUBIII. The first row shows cells from the 30HU-002 (NORM) cell line, the second from the 30HU-004 (sALS) cell line, the third from the CS52iALS-C9n6 cell line, and the fourth from the Cs04iALS-SOD1H44Rn3 cell line. Scale bar = 50 $\mu$ m.	49
4.12	Differentiation Efficiency of iPSCs into MNs across four different cell lines: 30HU-002 (NORM),	

30HU-004 (sALS), CS52iALS-C9n6, and Cs04iALS-SOD1H44Rn3, respectively.....	50
4.13 Average Neurite Length of MNs derived from four different cell lines: 30HU-002 (NORM), 30HU-004 (sALS), CS52iALS-C9n6, and Cs04iALS-SOD1H44Rn3, respectively .....	52
4.14 ChAT expression levels in four different cell lines: 30HU-002 (NORM, N), 30HU-004 (sALS), CS52iALS-C9n6 (CS52), and Cs04iALS-SOD1H44Rn3 (SOD1), respectively. The first two bands correspond to the control sample (labeled as 0) and the sample without reverse transcriptase (labeled as -RT), respectively .....	53

## List of Abbreviations

**Ach** – acetylcholine

**AFP** - Alpha Fetoprotein

**ALS** – Amyotrophic Lateral Sclerosis

**ASCs** - Adult Stem Cells

**BBB** - Blood-brain barrier

**bFGF** - basic Fibroblast Growth Factor

**bHLH** - basic-helix-loop-helix

**BDNF** - Brain-Derived Neurotrophic Factor

**BMP** - Bone Morphogenic Protein

**C9ORF72** - chromosome 9 open reading  
frame 72

**CCHC** - Cysteine-Cysteine-Histidine-Cysteine

**ChAT** - Choline Acetyltransferase

**CNTF** - Ciliary Neurotrophic Factor

**CNS** – Central Nervous System

**c-Myc** - Cellular myelocytomatosis oncogene

**CSD** - Cold Shock Domain

**CST** - Corticospinal tract

**CWS** - Column Wash Solution

**DMEM:F12** - Dulbeco’s Modified Eagle’s  
Medium/Nutrient Mixture F12

**DIV** – Day in vitro

**EAAT2** - Excitatory Amino Acid Transporter  
2

**EB** - Embryoid Body

**EMT** - Epithelialmesenchymal transition

**ESCs** - Embryonic Stem Cells

**FGF** - Fibroblast Growth Factor

**FLT1** - Vascular Endothelial Growth Factor  
receptor 1

**FOXA2** - Forkhead Box Protein A2

**FTD** - Frontotemporal dementia

**FUS** – Fused in sarcoma

**GFAP** - Glial Fibrillary Acidic Protein

**GFs** – Growth Factors

**HB9** - Homeobox HB9

**hPSCs** – human Pluripotent Stem Cells

**HSCs** - Hematopoietic Stem Cells

**ICM** - Inner Cell Mass

**IGF-1** - Insulin-like Growth Factor 1

**ISL-1** - Islet-1

**Klf4** - Kruppel-like factor 4

**LATE** – limbic predominant age-related TDP-  
43 encephalopathy

**Lin28** - Lineage Negative 28

**LMN** – Lower Motor Neuron

**MAP2** - Microtubule-associated protein 2

**MMPs** - Matrix metalloproteinases

**MND** – Motor Neuron Disease

**MN** – Motor Neuron

**MNPs** - Motor Neuron Precursors

**MSCs** - Mesenchymal Stem Cells

**NANOG** - Homeobox protein NANOG

**NCCs** - Neural Crest Cells

**NESTIN** - Neuroepithelial Stem Cell Protein

**NSCs** - Neural Stem Cells

**Oct4** - Octamer-binding transcription factor 4

**OLIG2** - oligodendrocyte transcription factor  
2

**PAX6** - Paired Box Protein Pax-6

**PBS** - Phosphate-buffered saline

**PDX1** - Pancreatic and Duodenal Homeobox 1

**PFA** - Perfluoroalkoxy alkane

**PGC** - Preganglionic column

**PLS** – Primary Lateral Sclerosis

**PMA** – Progressive Muscular Atrophy

**PNS** – Peripheral Nervous System

**RA** - Retinoic Acid

**RT** - Reverse Transcriptase

**RT-PCR** - Reverse Transcription Polymerase  
Chain Reaction

**RUNX1** - Runt-related transcription factor 1

**RWA** - RNA Wash Solution

**S.E.M.** – Standard Error of the Mean

**SeV** - Sendai Virus

**SHH** - Sonic Hedgehog

shRNA - short hairpin RNA

**SMAD** - Suppressor of Mothers Against  
Decapentaplegic

**SMN** – Somatic Motor Neuron

**SOD1** - superoxide dismutase 1

**Sox2** - Sex determining region Y-box 2

**SOX1** - SRY (sex determining region Y)-box  
1

**TARDBP/TDP-43** - TAR DNA-binding  
protein 43

**UMN** – Upper Motor Neuron

**Wnt** – Wingless-related integration site

**βTUB** - Beta-tubulin



# 1 Motivation

Neurodegenerative diseases are a group of disorders defined by the gradual deterioration of the structure and function of the nervous system [4]. These conditions affect millions of people and place a heavy burden on healthcare systems worldwide, accounting for a significant share of mortality and morbidity [3], [6]. These diseases are characterized by their complexity and heterogeneity, and they include Alzheimer's disease, Parkinson's disease, Huntington's disease, and Amyotrophic Lateral Sclerosis (ALS) [4]. Understanding the underlying mechanisms of these diseases is crucial to develop efficient therapies.

ALS, also known as Lou Gehrig's disease, is a neurodegenerative disease characterized by the loss of motor neurons in the brain, brainstem, and spinal cord [4]. ALS patients usually experience symptoms such as muscle weakness, atrophy, and eventual paralysis [4], resulting in death within 3 to 5 years following the diagnosis, typically due to respiratory failure [3]. There are two main categories of the disease: familial ALS (fALS), with a known family history of the disease, representing approximately 10% of cases; and sporadic ALS (sALS), with no known family history, accounting for the remaining 90% of cases [2], [3], [4], [7].

Various techniques have been used in order to uncover the diseases' pathophysiology and develop potential therapeutic options. Among these studies, genetic analysis was essential to identify mutations associated with fALS including those in the *SOD1*, *TARDBP* and *C9ORF72* genes [4], [2]. These findings have raised the possibility of generating transgenic animals, invaluable models for mechanistic and pharmacological investigations. Furthermore, several characteristics of ALS have been identified in *postmortem* analysis, such as the presence of protein aggregates like TDP-43 in affected tissues and the loss of motor neurons [3], [6].

Advancements in stem cell technology have provided numerous possibilities for ALS studies. Patient somatic cells can be reprogrammed into Induced Pluripotent Stem Cells (iPSCs) and subsequently differentiated into a wide range of neural cell types [8]. These iPSC-derived models offer a foundation for studying disease pathways within a specific context and for screening potential treatments. Consequently, the development of iPSC-based models can provide a greater understanding of the cellular and molecular changes linked to ALS in a controlled laboratory environment, which is crucial for the study of disease progression and the possible identification of novel targets for therapeutic intervention [9].

In this study, three different lines of iPSC-derived cells from ALS patients were used: one sALS line, two fALS lines with mutations in the *C9ORF72* and *SOD1* genes, and a control line from a healthy individual (NORM). These cell lines were differentiated using a protocol documented in the literature and adopted by the host laboratory with some modifications [10]. These iPSCs were used to develop disease models that mimic the cellular environment of ALS, allowing for the investigation of the disease mechanisms *in vitro* and the identification of possible treatment approaches.

The use of different iPSC lines, which encompass both familial and sporadic variants of the disease, allows for a thorough investigation of the genetic and phenotypic variability of ALS. The aim of this work is to better understand the shared and distinct mechanisms of ALS through the comparison of the morphological and functional characteristics across various lines. This approach improves our knowledge of the disease and also allows for the development of personalized therapeutics designed for each patient's genetic background.

In conclusion, the combination of advanced stem cell technologies with ALS research allows a better comprehension of the intricate nature of this disease. Through the employment of patient-derived iPSCs for precise disease modeling, it is possible to explore novel therapeutic approaches and work towards efficient ALS treatments, leading to an improvement in the quality of life of affected patients.

## 2 Introduction

### 2.1 Structure of the Nervous System

The nervous system consists of two compartments: the central nervous system (CNS), composed of the brain and spinal cord; and the peripheral nervous system (PNS), which includes all the nervous tissue outside the CNS (nerves and ganglia) [11], [12].

In terms of functionality, the PNS acts as an interface between the CNS and the different body structures, allowing the transmission of information and commands. The sensory division, also referred to as the afferent division, is responsible for transmitting action potentials<sup>3</sup> from the sensory receptors to the CNS. Neurons responsible for this function are termed sensory neurons. The motor division, also known as the efferent division, is responsible for conducting action potentials from the CNS to effector organs, which include muscles and glands. Neurons that undertake this task are called Motor Neurons (MNs) [12].

Additionally, the motor division can be subdivided based on the kind of effector that is being innervated: the somatic nervous system conveys action potentials from the CNS to the skeletal muscles, and the autonomic nervous system conducts action potentials from the CNS to the cardiac muscle, smooth muscle, and glands. The autonomic nervous system can be further subdivided into sympathetic and parasympathetic divisions, each with different functions [12].

### 2.2 Neuron Structure

The basic structural unit of the nervous system is the neuron. Neurons conduct nerve impulses from one part of the body to another. They have many specific characteristics, such as high metabolic rate, extreme longevity and they are typically nonmitotic (unable to divide and produce new neurons). There are many types of different neurons, but all of them share certain basic structural features, such as a cell body, dendrites and an axon. The cell body is the neuron's control center and is responsible for receiving, integrating and sending nerve impulses. It is enclosed by a plasma membrane and contains cytoplasm surrounding the nucleus. The nucleus contains a prominent nucleolus, showing the high metabolic activity of neurons. Dendrites are small processes that branch off the cell body. Nerve impulses are conducted by dendrites toward the cell body in order to be processed. The more dendrites a neuron has, the more nerve impulses that neuron can receive from other cells. An axon is a long nerve cell process emanating from the cell body. Neurons can have one or no axon at all, but usually they have one. It transmits a electrical impulse away from the cell body toward another cell [11].

Neurons can be classified according to their structure and to their function. Structurally, neurons can be classified based on the number of neuron processes emanating from the cell body: unipolar (a single process emerges from the cell body), bipolar (two neuron processes extend from the cell body) and multipolar (multiple neuron processes extend from the cell body). Regarding their function, neurons can be classified according to the direction of the nerve impulse travels relative to the CNS: sensory neurons (nerve impulses travel from sensory receptors to the CNS), MNs (Figure 2.1, nerve impulses travel from CNS to muscles and glands) and interneurons (they lie entirely within the CNS; they retrieve and store information and "decide" how the body responds to stimuli) [11], [12].

---

<sup>3</sup>Action Potentials: Also known as nerve impulse, is the rapid movement of an electrical charge along a neuron's plasma membrane.

The nerve impulse's ability to travel along an axon is affected by a process called myelination (process by which part of an axon is wrapped with a myelin sheath, the insulating covering around the axon consisting of concentric layers of myelin). The myelin sheath supports, protects, and insulates an axon. The small spaces interrupting the myelin sheath are called neurofibril nodes or nodes of Ranvier. At these nodes, a change in voltage may occur across the plasma membrane, resulting in a movement of the electrical impulse. Thus, this impulse seems to "jump" from one neurofibril node to another in a process called "saltatory conduction". In an unmyelinated axon, the electrical impulse must travel the entire length of the axon membrane, a process called continuous conduction. A myelinated axon produces a faster and more efficient impulse because only the exposed membrane regions are affected as the impulse jumps toward the end of the axon [11], [12]. In an unmyelinated axon, an electrical impulse takes longer to reach the end of the axon because every part of the membrane must be affected by the voltage change. Therefore, a myelinated axon requires less energy in the form of ATP than an unmyelinated axon to transmit the action potential [11].

## 2.3 Motor Neuron

As mentioned in Section 2.2, MNs are neuronal cells located in the CNS and are responsible for the innervation of effector muscles and glands, traveling through the complex circuits of the body in order to control both voluntary and involuntary actions. This synchronization is attained through a complex two-neuron circuit composed of upper MNs (UMNs), presenting the cell body in the cerebral cortex, and lower MNs (LMNs), with the soma located in the brainstem and spinal cord, which work together to produce a neural circuit that enables signals from higher brain centers to be transmitted to the muscles and glands. This intricate interaction ensures the smooth coordination of body movements [13], [14].

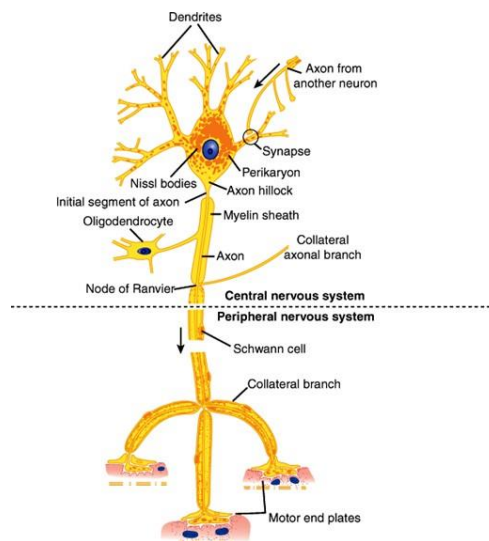


Figure 2.1: Schematic representation of a Nissl-stained motor neuron [4].

### 2.3.1 Upper MNs

UMNs are located in the pre-motor and primary motor regions of the cerebral cortex and they establish glutaminergic connections with LMNs within the CNS. Uncontrolled movements, reduced sensitivity to

superficial reflex stimulation, and the development of spasticity are among the clinical symptoms of UMN lesions [15].

### 2.3.2 Lower MNs

Similarly to upper MNs, lower MNs cell bodies are situated within the CNS and are found in specific nuclei within the brainstem and the ventral horn of the spinal cord. The distinctive characteristic of LMNs is their exceptional axonal extension and connection outside the CNS. These neurons are cholinergic neurons that receive information from upper MNs, sensory MNs, and interneurons. The effector muscle is then innervated by the lower motor neuron, enabling a rapid muscle response. A reflex arc promotes the immediate interpretation and reaction to a stimulus through the spinal cord, bypassing the brain, which leads to a faster effector response [13], [14], [16]. The clinical presentation of lower motor neuron lesions usually results in paralysis since there are no alternative means to send information to the peripheral muscle targets once these neurons are damaged. Lower MNs can be divided into three groups based on the type of target they innervate: branchial, visceral, and somatic MNs [13].

**Branchial MNs** Branchial MNs are situated in the brainstem and, together with sensory neurons, work to produce cranial nuclei. The trigeminal (V), facial (VII), glossopharyngeal (IX), vagus (X), and accessory (XI) nerves are the five cranial nuclei through which these MNs innervate the muscles derived from branchial arches in the face and neck [14]. Even though they serve a similar function to that of other skeletal muscles, the ones of the neck and face differ in their embryological origin. In contrast to the majority of the skeletal muscles, which derive from the somites<sup>4</sup>, the muscles in the neck and face originate from the branchial arches [13], [18].

**Somatic MNs** Somatic MNs (SMNs) are located in the Rexed lamina IX of the brainstem and spinal cord. SMNs are fundamental to the innervation of skeletal muscles, essential for movement [19]. These neurons constitute what is referred to as motor neuron pools: distinct groups that form connections with specific muscle targets. Three types of SMNs can be distinguished: alpha, beta, and gamma MNs [13].

**Alpha MNs** Alpha MNs are exclusively responsible for innervating extrafusal muscle fibers, playing a crucial role in muscle contraction. They are characterized by a large cell body and a distinct neuromuscular ending, making them a crucial component of the spinal reflex system. They receive monosynaptic innervation directly from sensory neurons (SNs), which reduces reaction latency [20]. This direct connection allows for rapid and efficient communication, making it easier for quick responses to occur during reflex activities [13], [21], [14].

**Beta MNs** Beta MNs, when compared to the other SMNs, are smaller and rarer. In contrast to other SMNs, beta MNs have a unique role as they innervate both extrafusal and intrafusal muscle fibers [22].

---

<sup>4</sup> Somites: Somites are repeated units with equivalent identities that are crucial to the vertebrate development and play a key role in forming the shape of the vertebrate body. These distinct structures emerge in pairs inside the presomitic mesoderm, illustrating a fundamental aspect of vertebrate mesodermal segmentation. Somites contribute to the development of several tissues, such as skeletal muscle, dermis, and sclerotome [17].

This unique characteristic differentiates beta MNs from the typical homogeneity found in motor units<sup>5</sup>. As they innervate both muscle fiber types, they have the ability to regulate both muscle contraction and the responsiveness of sensory feedback from muscle spindles [13], [21],[14].

**Gamma MNs** Gamma MNs have a crucial role in regulating the sensitivity of muscle spindles in the neuromuscular system. They are unique among SMNs since they only modulate the tension of intrafusal muscle fibers. Their firing pattern is designed to replicate the stretch experienced by the entire muscle by raising the tension in these specific muscle fibers. Gamma MNs have no direct motor function and only receive indirect sensory input. As a result, gamma MNs do not actively participate in spinal reflexes but considerably contribute to the modulation of muscle contraction [20], [13], [21],[14].

**Visceral MNs** Visceral MNs are an essential part of the autonomic nervous system (ANS), and they are responsible for controlling glands and smooth muscles, such as the arteries. The ANS can be divided into two parts: the ganglionic neurons, located in the peripheral nervous system (PNS); and the preganglionic MNs, situated in the CNS, connected to the ganglionic neurons. Furthermore, in anatomical and functional terms, the ANS can be divided into two different structures: the sympathetic and parasympathetic nervous systems [13], [14].

**Sympathetic MNs** The sympathetic nervous system is responsible for the mobilization of stored energy, increasing the level of awareness, and initiating an activation of the body's metabolism. The sympathetic MNs are located in the spinal cord, forming the preganglionic column (PGC). They are connected to three different targets: paravertebral and prevertebral ganglia adjacent to the spinal cord, and cells of the adrenal medulla. The latter is responsible for releasing catecholamines, such as adrenaline and noradrenaline, into the bloodstream in response to stress stimuli. Simultaneously, paravertebral and prevertebral ganglia connect to various targets, including the kidneys, intestines, colon, heart, and lungs [13].

**Parasympathetic MNs** The parasympathetic nervous system controls sexual behavior, stimulates the gastrointestinal tract, and regulates glandular production. The parasympathetic MNs are situated in two different regions: in the brainstem, promoting the development of the III, VII, IX, and X cranial nerves; and in the sacral segments of the spinal cord, which innervate ganglia near the peripheral targets, including kidneys, pancreas, bladder, lungs, and heart [13].

Information is transmitted from the CNS to the ganglionic neurons in the PNS through visceral MNs. Subsequently, these ganglionic neurons exert antagonistic control over a wide range of various visceral targets. Visceral MNs can be set apart from branchial MNs, which innervate muscles of the face and neck, and somatic MNs, responsible for skeletal muscle innervation, because they exhibit a unique feature: they do not form any connections with the final effector. Consequently, they represent an anatomical and functional exception among lower MNs [13].

---

<sup>5</sup>Motor Unit: A motor unit is composed of a motor neuron and all the myofibers it innervates [23].

## 2.4 Amyotrophic Lateral Sclerosis (ALS) as a Motor Neuron Disease

Nervous System Diseases have a wide variety of origins, such as degenerative, metabolic, structural, neoplastic, or inflammatory problems that affect neurons, glia<sup>6</sup>, or both. Functional aberrations arise from this diverse range of pathogenic pathways, which might show up as reduced neuronal function following a stroke or as increased neuronal activity, as seen in seizures. The particular brain network that is affected determines the nature of these functional abnormalities. For example, neurological impairments specific to the motor system occur as a result of ALS, which primarily affects upper and lower MNs. On the other hand, signs of extrapyramidal motor system dysfunction are brought on by the loss of dopaminergic neurons in the substantia nigra<sup>7</sup>, which is the characteristic feature of Parkinson's disease. In ischemic stroke patients, the group of deficits is intrinsically associated with the vascular region under distress. Therefore, a thorough comprehension of the pathophysiology of neurologic disorders requires a careful examination of events unfolding both within the complex architecture of neuronal networks and at the cellular level [4].

Motor Neuron Diseases (MNDs) predominantly target the anterior horn cells of the spinal cord, resulting in a distinctive clinical presentation characterized by muscular wasting and weakness. The pathophysiological manifestation includes spontaneous discharges from degenerating motor nerve fibers, giving rise to observable muscle twitches known as fasciculations. Electromyography analysis typically reveals denervation features, such as an increased occurrence of spontaneous discharges (fibrillations) in resting muscles and a reduction in the number of motor units detected during voluntary contraction [4].

Furthermore, the phenomenon of sprouting may occur among the remaining healthy motor fibers, leading to the emergence of large, polyphasic motor unit potentials indicative of reinnervation [3], [28]. MNDs have a broad age range of onset, typically ranging from 20 to 80 years, with an average initiation age of 56 years. While most cases are sporadic, approximately 10% of cases manifest familial occurrences. Different subtypes can be distinguished based on the major involvement of upper or lower MNs and bulbar or spinal anterior horn cells [4].

The most prevalent form of MNDs in adults is ALS, which presents with a confluence of upper and lower motor neuron deficits affecting limb and bulbar muscles [4]. ALS has a global annual incidence of 1-2.6 cases per 100 000 people, with an overall prevalence of 6 cases per 100 000, varying with age [3], [6]. The average age of ALS onset ranges between 58 and 60 years, and the average survival time from onset to death ranges between 3 and 4 years [3]. Sporadic ALS (sALS) constitutes an estimated 90% of cases, with the remaining 10% classified as familial ALS (fALS) [2], [3], [7], [4]. The latter is frequently observed in families with one or more first- or second-degree relatives or in people who have a known mutation in a disease-causing gene present in the family line [3].

---

<sup>6</sup> Glia: Also referred to as glial cells or neuroglia, these are non-neuronal cells in the peripheral and central nervous systems. Their functions include preserving homeostasis, promoting the development of myelin, and providing essential support and protection to neurons [24], [25], [26].

<sup>7</sup> Substantia Nigra: It is a basal ganglia localized in the midbrain, responsible for motor functions and reward processing. Its unique coloring is a result of the high levels of neuromelanin present in dopaminergic neurons [27].

### 2.4.1 Pathophysiology of ALS

In up to 90% of cases, considered to be sporadic, *postmortem* neuropathological examination of ALS tissues reveals distinctive characteristics, which include the selective loss of large MNs in the motor cortex, brainstem, and anterior horns of the spinal cord. Besides, it is possible to observe in myelin stains the thinning and scarring of lateral funiculi as a result of degeneration of corticospinal tract (CST) neurons. This loss of MNs causes the ventral roots to narrow and denervation atrophy (amyotrophy), affecting the muscles of the tongue, mouth, and limbs [3], [28]. Several mechanisms have been proposed to underlie motor neuron degeneration in ALS based on mechanistic and morphological observations. These include:

**TDP-43** Aggregates of hyperphosphorylated nuclear TAR DNA-binding protein 43 (TDP-43) are a pathological characteristic of ALS. One of the main components of the pathophysiology in ALS-TDP is the ubiquitinated inclusion, which occurs when TPD-43 suffers cleavage and mislocalization to the cytoplasm of MNs and glial cells [3], [29], [30]. This phenomenon correlates to the sequential propagation pattern along motor pathways, which supports the hypothesis of corticofugal propagation of misfolded proteins in ALS [3], [29]. Moreover, the cytoplasmic aggregation of TDP-43 occurs simultaneously with the loss of normal-associated immunoreactivity, with large neurons in the primary motor cortex being most affected [3], [31]. The accumulation of neurofilaments, which appear as spheroids or argyophilic structures, adds another layer to ALS pathology. These formations, which correspond to chromatolysis cytoplasmic alterations, result from phosphorylated neurofilaments in the proximal portion of the LMN axons [3].

**Glutamate Signaling and RNA Processing** The removal of glutamate from synapses involves transport proteins found on astrocytes and nerve terminals. Glutamate transport is significantly reduced in sporadic ALS patients, particularly in the motor cortex and spinal cord. This reduction is linked to the loss of the astrocytic glutamate transporter protein, Excitatory Amino Acid Transporter 2 (EAAT2). It has been proposed that a defect in the splicing of the messenger RNA EAAT2 is the possible cause of this loss. Additionally, it has been found that spinal MNs in ALS patients have a substantial modification in glutamate signaling. The process of RNA editing, which includes the modification of gene-specified codons by RNA-dependent deaminases, is generally very effective in the GluR2 subunits of the AMPA receptors. In this editing process, a glutamine in the second transmembrane domain is changed to an arginine, which substantially decreases the calcium permeability of AMPA receptors. In fact, more than 50% of ALS patients' neurons have been identified to have reduced RNA editing efficiency [4].

**Free Radicals** Approximately 20% of fALS cases are attributed to missense mutations in the cytosolic copper-zinc superoxide dismutase (*SOD1*). *SOD1* catalyses the conversion of the superoxide anion to hydrogen peroxide, which is subsequently detoxified to water by glutathione peroxidase, or catalase. Some mutations in *SOD1* lead to a reduction of its enzymatic activity, while others do not. Considering that familial ALS is usually inherited as an autosomal dominant trait, it is possible that *SOD1* function is gained rather than lost. Some observations prompted the conclusion that mutations in *SOD1* can cause hydroxyl radicals and tyrosine residue nitration by changing the substrate selectivity. Free radicals produced by mutant *SOD1* can inactivate the astrocytic glutamate transporter EAAT2 [4], and this can promote excitotoxicity. In addition, some mutations favor the formation of SOD aggregates, which could possess neurotoxic properties [4].

**Cytoskeletal Proteins** MNs are characterized by their substantial size, extensive axonal length, and the critical involvement of cytoskeletal proteins in maintaining axonal structure. A major contributing factor to motor neuron injury is damage to these proteins. Therefore, early neurofilamentous inclusions in cell bodies and proximal axons are associated with neurofilament dysfunction in ALS. Another significant factor is peripherin, an intermediate protein filament that coexists with neurofilaments in neuronal inclusions in ALS and in mice with *SOD1* mutations. In response to cellular injury, peripherin expression is increased, and the overexpression of peripherin has been linked to the development of late-onset motor neuron disease in mice. The inclusions containing peripherin and neurofilaments may interfere with axonal transport, which could compromise axonal structure maintenance and inhibit the transport of vital macromolecules, such as neurotrophic factors crucial for the survival of MNs [4].

***C9ORF72*** Researchers have discovered that hexanucleotide repeats in the *C9ORF72* gene, located on chromosome 9, can be found in 34% of familial ALS and 6% of sporadic ALS cases. The gain-of-function mechanism that these mutations cause can be compared to that of other noncoding repeat expansion diseases. These findings provide a strong justification for a novel drug development paradigm. Specifically targeting these toxic repeats' reduction appears to be a relevant direction for therapeutic exploration [4].

#### **2.4.2 Clinical Presentation**

In 80% of patients, initial symptoms manifest as limb muscle weakness, often bilaterally but with asymmetry. Bulbar muscle involvement results in challenges related to swallowing, chewing, speaking, breathing, and coughing. Neurological examination typically reveals an amalgamation of upper and lower motor neuron signs, with notable sparing of extraocular muscles and sphincters. The disease follows a progressive trajectory and is generally fatal within a span of 3–5 years, commonly attributed to complications such as pulmonary infection and respiratory failure [4].

There are several diseases within the ALS' clinical spectrum, each defined by the contribution of specific MNs and affected body regions. Examples include Primary Lateral Sclerosis (PLS), characterized by the isolated impairment of corticospinal MNs, and Progressive Muscular Atrophy (PMA), which can be defined by the involvement of spinal MNs alone [3], [32], [33].

ALS symptoms may differ based on the primary involvement of corticospinal neurons, the brainstem, or spinal cord MNs. For instance, early impairment of spinal cord neurons manifests as atrophy and asymmetrical weakness. Muscle cramping accompanies focal fasciculations that appear distally in the arms and legs after voluntary movements, such as stretching in bed. Regardless of whether the initial disease affects UMNs or LMNs, both eventually are affected. However, even in advanced stages of the disease, sensory, bowel, visual, and cognitive functions may remain intact [3].

#### **2.4.3 Genetic Basis of ALS**

Approximately 10% of sporadic ALS (sALS) and 60% of familial cases (fALS) are caused by pathogenic variants in the most common ALS-associated genes: superoxide dismutase 1 (*SOD1*), TAR DNA-binding protein (*TARDBP*), fused in sarcoma (*FUS*), and chromosome 9 open reading frame 72 (*C9ORF72*) [2].

**SOD1** A major turning point in the study of ALS was the identification of the SOD1 gene, which was linked to chromosome 21q in certain fALS pedigrees [34], [2]. *SOD1* is a copper-containing, low-molecular-weight cytoplasmic protein that functions as an antioxidant enzyme. This enzyme is essential for metabolizing superoxide radicals into molecular oxygen and hydrogen peroxide, protecting cells from their negative impact [35], [2]. It can be found in both mouse and human spinal cords in a variety of neural components, including MNs, interneurons, sensory neurons, and glial cells [36], [2]. Additionally, *SOD1* is expressed widely and abundantly, suggesting that pathogenic mutations in *SOD1* cause a toxic gain of function rather than haploinsufficiency [2]. Approximately 20% of fALS cases have *SOD1* mutations, with well-known mutations such as D90A, G93A, and A4V [37], [2]. These mutations cause changes in *SOD1* activity, which in turn causes pathological indicators linked to ALS such as protein misfolding, DNA degradation, and the accumulation of toxic hydroxyl radicals. Therefore, reducing the levels of toxic *SOD1* species is a therapeutic approach. Recent advancements in gene expression silencing techniques offer promising possibilities for the mitigation of *SOD1*-related ALS [2]. It is evident that there is clinical diversity among the different *SOD1* mutations, each presenting a characteristic phenotype. Through processes of excitotoxicity, oxidative stress, non-cell-autonomous toxicity of neuroglia, mitochondrial malfunction, and axonal transport disruption, the toxic gain of function demonstrated by mutant *SOD1* may lead to neuronal cell death [38], [3].

**TARDBP** A major breakthrough in the understanding of ALS pathology was the identification of TAR DNA-binding protein 43 (TDP-43). This discovery established an important connection between TDP-43 dysfunction and ALS pathogenesis by demonstrating that there was cytoplasmic accumulation and nuclear depletion of TDP-43 in the MNs of ALS patients [29], [3]. Furthermore, mutations in the *TARDBP* gene (encoding TDP-43) were identified as the cause of autosomal dominant ALS [39], [40], [3]. TDP-43 mutations can be found in other neurodegenerative diseases such as frontotemporal dementia (FTD) and limbic-predominant age-related TDP-43 encephalopathy (LATE) [41], [3]. Given that TDP-43 is an RNA-binding protein, motor neuron degeneration was proposed to be associated with RNA processing dysregulation [42], [43], [2]. The *TARDBP* gene encodes a nuclear RNA/DNA-binding protein that is involved in several RNA processing and metabolism functions [44], [3]. TDP-43 is mislocalized from the nucleus to the cytoplasm as a result of pathogenic mutations in *TARDBP*, which can cause toxic events through both gain- and loss-of-function mechanisms [45], [3]. The diversity in the ALS phenotype, with different clinical profiles and survival outcomes, is linked to specific mutations. The coexistence of ALS and cognitive impairment shows the common pathological processes causing TDP-43 proteinopathy [3].

**FUS** After the discovery of *TARDBP* as a dysregulated RNA-binding protein, pathogenic variants were found in another RNA-binding protein, Fused in Sarcoma (*FUS*) [46], [47], [46]. These variants account for 4% of familial and 1% of sporadic ALS cases and are primarily located in the C-terminal region, which is responsible for nuclear localization signaling [48], [49], [2]. Despite *FUS* mutations being usually linked to autosomal dominant ALS, cases of *de novo* mutations have also been reported [46], [50], [2]; these are frequently present in younger patients with a more aggressive course of the disease [51], [52], [53]. The clinical features of *TARDBP*-related ALS are also exhibited by *FUS* mutations, which include cytoplasmic aggregates and nuclear-to-cytoplasmic mislocalization of these proteins due to disruptions in RNA metabolism [46], [47], [52], [54]. In addition, stress

granules have recently been studied in the pathogenesis of ALS associated with *TARDBP* and *FUS* mutations. However, it is still unclear exactly how these contribute to the pathology of the disease [55], [56]. Mutations in the *FUS*-ALS gene are responsible for a significant loss-of-function in gene expression and splicing, directly affecting the amounts of intron retention in RNA-binding proteins. Further investigation into the pathogenic pathways of *FUS* mutations is necessary since these remain unclear [3].

***C9ORF72*** The *C9ORF72* gene has been identified as the most prevalent genetic cause of ALS and FTD. In European populations, this hexanucleotide repeat expansion can be found in 40% of familial and 7% of sporadic ALS cases [57], [2], and it can set affected individuals apart from the wild-type allele carriers with fewer than 30 repeats [58], [2]. There are contradictory findings about the relationship between expansion size and age at onset. Furthermore, a wide range of clinical presentations linked to *C9ORF72* repeat expansion have been described [59], [2]. Several mechanisms, such as nuclear RNA foci, repeat-associated non-AUG-initiated translation, toxic gain of function, and *C9ORF72* haploinsufficiency, have been proposed to explain *C9ORF72*-related neurodegeneration [60], [61]. However, more research is required to determine the precise cascade of events leading to neuronal death. FTD and/or ALS can be characterized by the heterozygous hexanucleotide repeat expansion in *C9ORF72*, constituting the most prevalent ALS-causing gene [58], [62]. Affected individuals show a wide spectrum of repeat lengths; symptoms may appear with as few as 20-22 repeats [63]. *C9ORF72* mutation carriers usually present with combined upper and lower motor neuron symptoms, and when compared to sporadic cases, they are more likely to experience bulbar-onset disease and frontotemporal dementia (FTD) [64], [3]. Furthermore, *C9ORF72*-related ALS exhibits bunina bodies, corticospinal tract degeneration, and ubiquitinated neuronal and glial cytoplasmic inclusions, characteristic of ALS-associated pathogenic proteins [3]. Table 2.1 summarizes the main characteristics of the four most common ALS-associated genes.

Table 2.1: Summary of the four most common ALS-associated genes [2], [3].

Gene	Chromosomal Locus	Inheritance Pattern	Familial (%)	Sporadic (%)	Function	Disease-associated mechanism	Other associated phenotypes
<i>SOD1</i>	21q22.11	Autosomal dominant, autosomal recessive, <i>de novo</i>	12	1-2	Protein antioxidant	Oxidative stress, excitotoxicity, mitochondrial dysfunction, axonal transport disruption	Frontotemporal dementia, spastic tetraplegia and axial hypotonia
<i>TARD BP</i>	1p36.22	Autosomal dominant, autosomal recessive, <i>de novo</i>	4	1	DNA, RNA binding	Altered ribostasis, nucleocytoplasmic transport defects	Frontotemporal dementia
<i>FUS</i>	16p11.2	Autosomal dominant, autosomal recessive, <i>de novo</i>	4	1	DNA and RNA metabolism, DNA repair, and regulation of transcription, RNA splicing, and export to the cytoplasm	Altered ribostasis, nucleocytoplasmic transport defects	Frontotemporal dementia, essential tremor
<i>C9OR F72</i>	9p21.2	Autosomal dominant	40	7	Regulates vesicle trafficking	Autophagy, global RNA alterations, intracellular trafficking defects, nucleocytoplasmic transport defects, proteostasis defects	Frontotemporal dementia

## 2.5 Stem Cells

Stem cells, crucial elements in modern biology, are widely recognized for their capacity for self-renewal and multilineage differentiation. Originating in the late 19th century, the term "stem cell" was initially used to describe germ-plasm continuity and the genesis of the hematopoietic system. While Ernst Haeckel introduced the term "Stammzelle" in 1868, it wasn't until nearly a century later, in the 1960s, that the definitive characterization of hematopoietic stem cells was achieved. This was due to the work of James Till and Ernest McCulloch, who discovered clonogenic bone marrow precursors capable of generating macroscopic spleen colonies upon transplantation into irradiated recipient mice [65], [9].

There are two characteristics that distinguish stem cells from other types of cells: self-renewal and potency.

Self-renewal can be described as the capacity of stem cells to divide and generate new stem cells. This process allows stem cells to remain undifferentiated throughout an organism's lifetime, therefore preserving the stem cell pool. A mother stem cell divides into one or two daughter cells, with at least one daughter cell retaining the capacity to develop similarly to the mother cell. The mechanisms of stem cell self-renewal involve both symmetrical and asymmetrical divisions. In the first one, the mother cell divides, producing two daughter cells that maintain the same developmental potential as the mother cell. On the other hand, asymmetrical cell division is the process in which daughter cells have different fates due to the disparity in the distribution of cell-fate determinants or environmental variations. These mechanisms are essential for

the expansion of stem cell numbers during development and maintaining tissue homeostasis in adult organisms. Dysregulation of these processes can result in premature aging phenotypes, cancer predispositions, and developmental abnormalities [66].

Conversely, potency refers to a cell's ability to differentiate into different cell types [66]. Regarding their differentiation potential, cells can be classified as:

**Totipotent Stem Cells** These cells possess the ability to differentiate into all cell types necessary for the full development of an organism, including the placental trophoblasts and embryos [67], [68].

**Pluripotent Stem Cells** These cells are capable of differentiating into a broad variety of cell types derived from all three germ layers (ectoderm, mesoderm, and endoderm), with the exception of the ability to form an entire organism [67].

**Multipotent Stem Cells** These cells are characterized by their capacity to develop into a limited variety of cell types, specific to the tissue in which they originated [67].

**Oligopotent Stem Cells** These cells can only differentiate into a small number of closely related cell types, having a more restricted differentiation potential when compared to multipotent stem cells [69].

**Unipotent Stem Cells** These are specialized cells capable of differentiating only into a single type of cell, maintaining a single lineage [68].

Considering all of this, it is clear that stem cells represent a major advancement in regenerative medicine and medical research. Their self-renewal and potency abilities offer new opportunities for comprehending disease mechanisms, developing innovative treatments, and improving patient outcomes. Furthermore, stem cells hold great promise for the treatment of a variety of conditions, including spinal cord injuries, cardiovascular diseases, and neurodegenerative diseases such as Alzheimer's and Parkinson's diseases. Additionally, they allow for personalized medicine, enabling treatment customization for each patient according to their particular genetic composition and disease characteristics [66].

Furthermore, stem cells hold a promise to study embryonic development, cellular differentiation, and organ maintenance, offering potential for innovative cell-based therapies [67], [65].

Therefore, stem cells have the potential to transform disease treatment and management, improving patient lives worldwide [67], [65].

Regarding their origin, a variety of stem cells are used in research, including embryonic stem cells (ESCs), adult stem cells (ASCs), and induced pluripotent stem cells (iPSCs). A shift in the field of regenerative medicine began in 1998 with the emergence of the first human embryonic stem cell lines [67].

**Embryonic Stem Cells** Embryonic Stem Cells (ESCs) are cells originating from the inner cell mass (ICM) of early blastocysts or primitive gonadal regions of aborted fetuses. They have the ability to differentiate into almost any type of cell that originates from the three germ layers. However, they cannot be considered totipotent since they are unable to form the placenta and supporting tissues, preventing them from giving rise to the entire embryo. Therefore, they are classified as pluripotent stem cells [65], [68].

Due to their self-renewal and pluripotency properties, ESCs are invaluable for early human embryogenesis studies and for the advancement of cell-based therapies in regenerative medicine. As a result of their embryonic developmental stage, they have a higher differentiation potential than adult stem cells, making them more suitable for large-scale *in vitro* cultivation for possible cell replacement therapies [9], [67].

In this manner, ESCs are the most versatile among stem cells; they have the capacity to significantly change the treatment course of a wide range of diseases, including diabetes, cancer, neurodegenerative conditions, and cardiovascular problems [65], [68].

In spite of their great potential for regenerative medicine, it is important to acknowledge the limitations and ethical concerns surrounding the use of ESCs. For instance, chromosomal abnormalities are common in mouse ESCs and embryonal carcinoma cells, probably potentiated by laboratory manipulations and requiring strict culture conditions and regular monitoring.

There are several ethical concerns with ESCs, particularly those associated with the use of human embryos for their derivation. This presents serious moral concerns regarding the status of early human embryos and the morality of using them for research. These ethical issues are further aggravated by global legislative discrepancies, with variations in acceptable practices and funding limitations. Some countries allow spare embryos to be used to create new cell lines, while others impose restrictions on federal funding based on the date the cell line was created [9], [67].

In addition, concerns about tissue rejection in ESC-based cell replacement therapies emphasize the necessity for extensive studies to ensure efficacy and safety. The requirement to produce pure specialized cell types is further underscored by the potential for tumor formation resulting from the presence of undifferentiated ESCs. Translating ESC research into therapeutic applications requires overcoming technical obstacles such as large-scale culture strategies and directed differentiation protocols [70].

**Adult Stem Cells** Adult stem cells (ASCs), also known as somatic stem cells [67], are undifferentiated cells found in differentiated tissues with limited capacity for self-renewal and differentiation. ASCs can be collected from the placenta, umbilical cord blood, and fetal tissues such as the liver and pancreas [70] and they include hematopoietic and mesenchymal stem cells.

Hematopoietic stem cells (HSCs) are known for their transdifferentiation potential, which is the ability to differentiate into various cell types. They are able to differentiate into a wide variety of cell types and overcome lineage barriers [68]. Furthermore, they are the basis of successful bone marrow transplantation and have been employed extensively in clinical settings for over 40 years [67]. HSCs are mostly responsible for hematopoiesis in the bone marrow and give rise to both myeloid and lymphoid lineages of blood cells [9]. In contrast, Mesenchymal Stem Cells (MSCs) differentiate into a variety of adult mesenchymal tissues, such as bone, cartilage, adipose tissue, and muscle, whereas hematopoietic stem cells, located in the bone marrow, differentiate into mature blood cells. MSCs have demonstrated potential for tissue repair, especially in the bones and joints. They are predominantly located in the bone marrow and are believed to produce daughter cells that develop into various mesodermal tissue types in response to local injury. The potential of ASCs for regenerative medicine is further emphasized by their plasticity, as both cell types can develop into cells from different organ systems [9].

However, ASCs pose difficulties for their usage in therapeutic applications since they are rare and difficult to isolate in large numbers from their *in vivo* niche<sup>8</sup> [9].

---

<sup>8</sup>Niche: microenvironment within a specific local tissue where stem cells are located. It supports and regulates a particular stem cell or progenitor. The niche controls tissue architecture and stem cell differentiation, which are crucial for development, tissue homeostasis, and organogenesis [9], [71].

**Induced Pluripotent Stem Cells** Induced Pluripotent Stem Cells (iPSCs) are a type of pluripotent stem cell that can be produced directly from non-pluripotent stem cells, such as adult somatic cells, through a process known as reprogramming [8]. Shinya Yamanaka and his team introduced a new approach in 2006 when they showed that adult cells could be induced into a pluripotent state similar to that of ESCs by the introduction of specific transcription factors [72].

iPSCs and ESCs have several shared characteristics, such as the capacity for self-renewal and differentiation into distinct cell types from all three germ layers. Due to their pluripotency, iPSCs can be a powerful tool in drug discovery, disease modeling, and regenerative medicine [9].

Furthermore, iPSCs have the advantage of holding patient-specificity since they can be derived from a person's own cells, which reduces the risk of immunological rejection in transplant settings. In this way, iPSCs have the potential to transform stem cell research by providing unprecedented customized therapy and broadening our knowledge of developmental biology and disease pathophysiology [67], [8].

Nevertheless, there are ethical concerns and limitations surrounding the use of iPSCs. The main ethical concern revolves around the source of iPSCs, usually generated by reprogramming adult cells, which raises concerns about donor exploitation and informed consent. Additionally, there are also concerns about genetic defects and tumorigenicity as a result of the reprogramming process, which pose risks for patient safety and effectiveness when used in transplants. Ethical concerns also extend to consent, privacy, and commercialization. In addition, iPSC production has some limitations in terms of genetic instability, possibility of tumor formation, high production costs, and accessibility concerns for patients [9], [67].

Table 2.2 summarizes the most important characteristics of ESCs, ASCs, and iPSCs.

Table 2.2: Summary of the most important characteristics of ESCs, ASCs, and iPSCs.

	<b>Embryonic Stem Cells (ESCs)</b>	<b>Adult Stem Cells (ASCs)</b>	<b>Induced Pluripotent Stem Cells (iPSCs)</b>
<b>Source</b>	Derived from ICM of early blastocysts or gonadal regions of aborted fetuses	Found in differentiated tissues, including bone marrow, umbilical cord, and fetal tissues	Reprogrammed from adult somatic cells
<b>Potency</b>	Highly pluripotent (can differentiate into almost any cell type)	Limited differentiation capacity compared to ESCs	Pluripotent (can differentiate into various cell types)
<b>Self-Renewal</b>	High self-renewal capacity	Limited self-renewal capacity	High self-renewal (can proliferate indefinitely)
<b>Potential for Large-Scale In Vitro Culture</b>	Suitable for large-scale <i>in vivo</i> cultivation	Difficult to isolate in large numbers from <i>in vivo</i> niche	Can be expanded <i>in vivo</i>
<b>Immunocompatibility</b>	Might cause immunological reaction due to foreign origin	Lower risk of immunological reaction when compared to ESCs	Reduced risk for immunological reaction due to its patient-specific nature
<b>Tumor Formation Risk</b>	Potential for tumor formation due to the presence of undifferentiated cells	Lower risk of tumor formation when compared to ESCs	Risk for tumorigenicity due to reprogramming process
<b>Ethical Considerations</b>	Derived from human embryos, raising ethical considerations regarding the moral status of early human embryos and their application in research	Rare and difficult to isolate in large numbers from their <i>in vivo</i> niche, posing ethical questions about donor exploitation and informed consent	Reprogrammed from adult cells, which involves adult donors, reducing the concerns about embryo use and donor exploitation
<b>Clinical Applications</b>	Early human embryogenesis studies and disease modeling	Widely used in current clinical therapies for various conditions, but limited when compared to ESCs and iPSCs	Drug discovery, disease modeling, and regenerative medicine research

## 2.6 Induced Pluripotent Stem Cells (iPSCs)

As described in Section 2.5, iPSCs represent a major breakthrough in stem cell research. In order to obtain iPSCs from somatic cells, a process of reprogramming must be undertaken. Reprogramming is the process of inducing pluripotency in adult somatic cells (already differentiated and non-pluripotent) by the controlled expression of specific transcription factors<sup>9</sup>. The differentiation properties of adult cells are modified during this process to resemble those of the undifferentiated embryonic state [74].

Reprogrammed adult somatic cells give rise to iPSCs, which share similar characteristics with ESCs, including pluripotency and the ability to differentiate into several mature cell types. This versatility makes iPSCs useful in disease modeling, drug discovery, and personalized therapy. Since the cellular source has a significant impact on the reprogramming efficiency, kinetics, and quality of iPSCs, it is essential to choose the most adequate starting somatic cell type in order to achieve efficient reprogramming. There are several characteristics that must be taken into consideration when selecting the somatic cell source, including [75]:

- Abundance of the somatic cell in the tissue [75];
- Accessibility of the somatic cell in tissue (ease of isolation using minimally invasive procedures) [75];
- Ability for cell culture and expansion in order to obtain a sufficient cell population for reprogramming within a short timeframe [75];
- Genetic stability (absence of critical somatic mutations and chromosomal aberrations), crucial for the maintenance of genomic integrity throughout the reprogramming process [75];
- Ability for a high-efficiency reprogramming process with fast kinetics [75];
- Reprogramming potential across different ages and pathological conditions [75].

A number of somatic cells can be used as starting material for the reprogramming process, including keratinocytes, urine cells, and peripheral blood mononuclear cells [75]. However, the most commonly used ones are fibroblasts<sup>10</sup>. There are some disadvantages to their use as a starting cell type, such as their relatively poor reprogramming efficiency, the need for unpleasant skin biopsies to obtain them, and the risk of newly reprogrammed cells proliferating too quickly due to overgrowth. Furthermore, fibroblasts should only be used at a very low passage, no higher than passage five, in order to preserve reprogramming efficacy and lower the risk of cumulative genomic alterations. On the other hand, there are several advantages associated with the use of fibroblasts that make them the most suitable candidate for starting cells in the reprogramming process. These include their high availability, ease of isolation from

---

<sup>9</sup>Transcription Factors (TFs): TFs are proteins essential for the regulation of gene expression because they control the transcription of genes in response to specific stimuli. The synthesis of these proteins can be regulated, and changes in their properties can result in a variety of diseases. TFs are crucial for normal development, tissue-specific protein synthesis, and the response to specific cellular signaling pathways [73].

<sup>10</sup>Fibroblasts: Spindle-shaped cells characterized by an oval, flat nucleus and primarily found in the interstitial spaces of organs [76]. Fibroblasts are fundamental constituents of the structural framework in animal tissues. Additionally, they are responsible for collagen and extracellular matrix (ECM) synthesis, thus constituting the most common type of connective tissue in animals. Fibroblasts are also involved in several physiological processes, including the facilitation of epithelial differentiation, the regulation of inflammation, and the promotion of wound healing [77].

skin biopsies, and ease of cultivation, propagation, and cryoconservation. In addition, when compared to other cell types, fibroblasts show a very high proliferation rate, which can be beneficial for the reprogramming process [78].

### 2.6.1 Reprogramming Factors

Several TFs have been identified as crucial in the reprogramming process. Four TFs, known as the Yamanaka factors, have been discovered by Yamanaka and colleagues: Oct4, Sox2, c-Myc, and Klf4 [72]. However, another set of TFs - OCT4, SOX2, NANOG, and LIN28 - has also been identified. These latter are known as the Thomson factors [79].

**Oct4 (Octamer-binding transcription factor 4)** *Oct4*, also known as *Oct3/4* [80], is encoded by the gene *Pou5f1* [81]. This transcription factor is essential for maintaining and regaining stem cell pluripotency, where it has at least three isoforms (OCT4A, OCT4B, and OCT4B1), with only OCT4A preserving stemness in pluripotent stem cells [82]. Oct4 is a member of the POU transcription factor family and binds an octameric sequence motif (with the AGTCAAAT consensus sequence) to regulate the expression of target genes [82]. Its precise expression level is crucial for embryonic stem cell fates, and their pluripotent potential can be maintained only when the Oct4 expression level remains within a normal range. Oct4 overexpression leads to the development of primitive endoderm and mesoderm, whereas a reduction in its expression results in differentiation into trophoblasts [82]. Oct4 is regulated at multiple levels, such as chromatin modification, transcriptional regulation, post-transcriptional regulation, and post-translational modifications. In combination with other pluripotency factors, it defines the state of pluripotency in embryonic stem cells [82].

**Sox2 (Sex determining region Y-box 2)** Sox2 is a transcription factor essential for maintaining pluripotency in mouse embryonic stem cells. It regulates the expression of transcription factors that affect Oct3/4 expression, assisting Sox2-null ES cells in retaining their pluripotency [83]. This suggests that Sox2 has an important role in stabilizing pluripotency by preserving Oct3/4 levels. As it modulates nuclear receptor family members including Nr5a2 and Nr2f2, Sox2 indirectly influences Oct3/4 expression, thus blocking ESCs' differentiation [83]. Among its diverse range of roles are tumorigenesis, regulation of embryonic and adult stem cell self-renewal, and the generation of iPSCs. Elevated levels of Sox2 in cancer scenarios are associated with poor prognosis, cancer stem cell proliferation, and resistance to therapy [84].

**c-Myc (Cellular myelocytomatosis oncogene)** c-Myc is an oncogenic transcription factor essential in tumorigenesis. It combines the cell cycle mechanism with cell adhesion, cellular metabolism, and apoptotic pathways as a result of gene, which can be caused by chromosomal translocations, gene amplification, and point mutations. Consequently, this can lead to a variety of cancer pleiotropal gene expression regulation [85]. Human cancers frequently have mutations in the c-Myc types [85]. Additionally, c-Myc plays a crucial role in embryonic development and cell growth, with targeted deletion of the mouse c-Myc gene resulting in embryonic mortality and inactivation of the gene extending cell doubling time in immortalized rat fibroblasts [86], [85].

**LIN28 (Lineage Negative 28)** LIN28 is an RNA-binding protein essential in both development and disease, especially in stem cell biology and cancer [87]. It was initially identified as a regulator of developmental processes during the early studies of the heterochronic pathway in *C. elegans* [88]. LIN28 can be characterized by the distinct combination of a cysteine-cysteine-histidine-cysteine (CCHC) zinc knuckle domain and a cold shock domain (CSD) [88], [87]. There are two paralogs in vertebrates: *Lin28a* and *Lin28b*. While a high sequence similarity between these proteins has been described, especially in their RNA-binding domains, there are differences concerning their subcellular localization and certain functional features. *Lin28a* is predominantly found in the cytoplasm, whereas *Lin28b* is located in the nucleus, specifically in the nucleolus [88]. LIN28's main function consists of regulating the microRNA let-7 (a key factor in the transition from an undifferentiated to a differentiated state), therefore promoting pluripotency. LIN28 inhibits the biogenesis of let-7, which preserves stem cells' pluripotency. Nevertheless, LIN28 has other functions, such as direct regulation of mRNA targets associated with cell cycle regulation, nuclear RNA-binding proteins, histone components, glucose metabolism, and early embryonic genes [88]. Regarding development, LIN28 is highly expressed in embryonic stem cells and inhibited during differentiation. Furthermore, it is crucial for tissue regeneration and iPSC reprogramming, where it increases the efficiency and promotes the proliferation of stem and transit-amplifying cell populations, which increases tissue size and repair. LIN28 is the only one among the initial reprogramming factors that is not a transcription factor [87]. Aberrant LIN28 expression has been linked to an array of cancers, stimulating the aggressive nature of tumors by promoting proliferation, invasiveness, and metastasis [88].

**NANOG (Homeobox protein NANOG)** NANOG is a transcription factor essential to self-renewal and to the undifferentiated state in ESCs [89]. This protein was first discovered in 2003 [79], and it was described to play a crucial role in pluripotency network regulation, together with Oct4 and Sox2. NANOG is also a key player in the reprogramming of somatic cells into iPSCs when combined with other reprogramming factors (Oct4, Sox2, and Lin28) [89]. Furthermore, this protein has also been identified as critical for the development of the inner cell mass in early embryos and for the maintenance of germ cell development [79]. NANOG has also been connected to several aspects of cancer biology. The phenotypic properties of cancer stem cells, which are believed to be the basis of tumor growth and metastasis, are shared with aberrant NANOG expression, which, consequently, is associated with the development of malignancy in cancer cells. More specifically, NANOG plays a role in cancer by promoting cell proliferation, epithelial-mesenchymal transition (EMT), apoptosis resistance, and metastasis [89]. Accordingly, the expression of NANOG is associated with a poor prognosis in several cancer types, such as gastric adenocarcinoma and colorectal cancer. Elevated levels of NANOG are linked to increased tumor invasion and metastasis and, as a consequence, a lower patient survival rate. In addition, it has been demonstrated that NANOG suppression reduces migration, invasion, and expression of matrix metalloproteinases (MMPs), which are enzymes involved in the destruction of the extracellular matrix and metastasis [89].

**Klf4 (Krüppel-like factor 4)** Klf4 is a transcription factor from the Sp/KLF family. It can be distinguished by the C-terminal DNA binding domain, which is homologous to the Sp1 protein. In addition, it is crucial for cell growth and differentiation, especially in epithelial and endothelial cells. It is a protein with a zinc finger DNA binding domain that enables it to interact with specific DNA sequences in target gene promoters [90], [91]. Furthermore, Klf4 presents a wide variety of functions, acting as a transcriptional activator or repressor, depending on the gene it interacts with. In addition, it is involved in the regulation of cell cycle progression and differentiation genes, interacting with other transcription factors and signaling pathways in order to optimize gene expression profiles [90]. Besides, Klf4 is one of the fundamental transcription factors used in iPSC reprogramming. It has been demonstrated to directly repress p53 (a tumor suppressor protein), which, subsequently, suppresses NANOG during embryonic stem cell differentiation. This suggests that, through the repression of p53, Klf4 may activate Nanog and other embryonic stem cell-specific genes. Finally, it has been shown, also through the repression of p53, that Klf4 can act as a Myc-induced apoptosis inhibitor, which could be critical for cell survival during the reprogramming process [92].

## 2.6.2 Reprogramming Methods

As mentioned in Section 2.6, the reprogramming process consists of inducing pluripotency in adult somatic cells through the controlled expression of specific transcription factors. In order to do this, there are a broad range of reprogramming approaches that can be used. Reprogramming methods are the techniques used to induce the transformation of somatic cells into iPSCs. They can be divided into two groups: integrating and non-integrating methods. In the integrating methods, transcription factors are introduced into the host cells by viral vectors (retroviruses and lentiviruses), inducing pluripotency. Nonetheless, these methods present some limitations, including the risk of insertional mutations and tumorigenesis. On the other hand, non-integrating methods reduce the risk of genetic modifications because they reprogram cells without integrating into the host genome. In order to achieve this, delivery vehicles such as episomal plasmids, transposons, and recombinant proteins are used in the reprogramming process. Furthermore, there are several small molecules and chemical compounds that are able to effectively reprogram cells by modulating their epigenetic status and targeting signal transduction pathways. The advantages of these methods include increased safety, reduced immunogenicity, and the potential for clinical-grade iPSC generation [93].

**Integrating Methods** Integrating Methods are the conventional technology in iPSC generation and were crucial in their early development. However, these methods present some disadvantages, including the risk of insertional mutagenesis, residual expression, and reactivation of reprogramming factors, which can lead to tumorigenesis [94].

**Retroviral and Lentiviral Transduction** Retroviral and lentiviral transduction were among the first methods used for the generation of iPSCs. In these techniques, the reprogramming factors (discussed in Section 2.6.1) are delivered into somatic cells through viral vectors that integrate these factors into the genome of the host cell, resulting in their constant expression and the induction of pluripotency. Nevertheless, as they integrate directly into the host genome, these techniques have a number of disadvantages, including the potential promotion of insertional mutagenesis, which can increase the risk of tumorigenesis, and the potential for malignant transformation, especially considering the pro-cancerous

role of c-Myc. Therefore, there are some limitations in its clinical applications [75]. On the other hand, they present other advantages. Lentiviral vectors, derived from HIV-1 [94], [75], can infect non-dividing cells, which makes them more efficient and has a broader tropism [95], [96].

**Inducible Lentiviral Methods** Inducible Lentiviral techniques, which allow for temporal control over the expression of reprogramming factors, have been developed in order to reduce the risks associated with retroviral and lentiviral transduction. These inducible techniques are regulated by doxycycline, and once reprogramming is complete, the factors' expression can be turned off, reducing the risk of insertional mutagenesis [95]. There is a technique known as the transgene excision method that involves the use of doxycycline-inducible lentiviral vectors with LoxP sites. After reprogramming, these sites can be removed by using the Cre-recombinase enzyme, so that the transgenes are eliminated. In spite of their lower efficiency, these techniques assist in mitigating some of the safety concerns associated with traditional retroviral and lentiviral transduction methods [75].

**Non-Integrating Methods** Non-integrating methods have been developed in order to mitigate the risks associated with genomic integration. Although less efficient, these methods are safer for clinical use [95].

**Episomal Vectors** Episomal Vectors are plasmids that are able to deliver reprogramming factors without integrating into the host genome [95]. This method is highly reliable for reprogramming fibroblasts and blood cells [96], and it has several advantages, including the fact that these plasmids are preserved in the cell as extrachromosomal elements and, after the conclusion of the reprogramming process, are eliminated [95]. However, the use of a TP53 short hairpin RNA (shRNA) cassette, which can potentially impact the stability and safety of the iPSCs, raises concerns regarding the genetic integrity of the resulting iPSC lines [96].

**Sendai Virus (SeV) Reprogramming** The SeV reprogramming method is a non-integrating method used to generate iPSCs by delivering reprogramming factors to target cells. It reduces the risk of genomic integration by replicating in the cytoplasm without a DNA intermediate. This technique involves using F-deficient SeV vectors (SeVV/DF) to efficiently reprogram different cell types. In order to enhance efficiency and safety, the vectors can be engineered to carry all four reprogramming factors (OCT4, SOX2, KLF4, and cMYC) in a single vector (SeVV/DMDFDHN). Since viral genomes are lost through cell division, it is possible to obtain transgene-free iPSCs by selecting against cells carrying viral genomes. This method is promising for clinical approaches due to its high efficiency and ability to generate transgene-free iPSCs [94], [96].

**Protein Reprogramming** Direct delivery of transcription factors, also referred to as protein transduction or protein reprogramming, can be described as the process of delivering the reprogramming factors directly into the cells without needing nucleic acid delivery [95], [75]. It is a non-genetic technique that eliminates the risks of genomic integration (concerns associated with integrating methods) [95], [94], [75]. However, this method has lower efficiency when compared to other techniques, and the production process of these proteins is difficult [75].

**Small Molecules and Chemical Reprogramming** Multiple techniques have been developed that make use of small molecules and soluble factors in order to improve the reprogramming process or eliminate the need for some transcription factors. These include histone deacetylase inhibitors, DNA demethylating agents, and different signaling molecules [95]. These compounds can be employed to

induce pluripotency by modulating various cellular pathways. Therefore, they can operate as independent pluripotency inducers, replace reprogramming factors, or enhance reprogramming efficiency [75]. Small molecule approaches have the advantage of being easier to control and not modifying the genome [95]. However, these techniques can be less efficient than genetic methods [94], [75].

### **DNA-Based Methods**

- PiggyBac transposon: This method provides a low-risk reprogramming process through the use of a mobile genetic element that can transpose between vectors and chromosomes without integration [75].
- Adenoviral vectors: These vectors have been used to generate iPSCs from a variety of cell types, but they do not integrate into the host genome. However, they are not as efficient at transduction as retroviral vectors [75].
- Non-viral minicircle DNA vectors: Minicircle DNA vectors are a type of plasmid DNA that do not contain bacterial backbone sequences, which makes them more efficient for transgene expression (guidelines). These vectors can be used in the reprogramming process of iPSCs without the potential risk of genomic integration [75],[95]. Similarly to other non-integrating techniques, this method prevents the complications associated with genomic integration at the cost of lower efficiency [75].

### **Non-DNA-Based Methods**

- mRNA reprogramming: Through this process, in vitro-transcribed mRNAs encoding the reprogramming factors are delivered to the cells, enabling their reprogramming with a reduced immunogenic response and without a genetic signature [75], [96]. However, daily transfections are necessary to guarantee the success of the process, as the mRNA is not integrated into the genome and has a very short half-life. Thus, although mRNA reprogramming is efficient, it can be difficult to perform due to the need for specialized equipment and the significant amount of work associated with the daily transfections [96].
- MicroRNA (miRNA) Reprogramming: In this technique, specific, non-coding miRNA clusters are used to reprogram somatic cells into iPSCs without the need for vector-based gene transfer. Since this method does not involve genome integration, it can be considered a safer approach, making it a viable strategy for clinical applications [94], [75].

When selecting a reprogramming technique, it is important to take into consideration that each has its own set of difficulties and limitations, including efficiency, safety, and particular requirements of the study or clinical application [95], [96]. Besides, the type of cell being reprogrammed and the aim of the study affect method selection [95]. The risks associated with genetic modification have decreased due to the development of non-integrating and non-DNA-based approaches, which increases the safety and potential for clinical use of iPSCs. Additionally, when selecting the most adequate approach, it is important to consider the advantages and limitations of each method in light of the specific demands of the project, such as cell therapy, disease modeling, or drug discovery [75]. Therefore, as the field of regenerative medicine advances, the aim is the continued development of safer and more efficient reprogramming techniques [95].

Table 2.3 summarizes the advantages and disadvantages/limitations of Integrating and Non-Integrating methods.

Table 2.3: Summary of the Advantages and Disadvantages/Limitations of Integrating and Non-Integrating Methods.

Method	Type	Advantages	Disadvantages/Limitations
Retroviral Transduction	Integrating	High Efficiency; Stable expression of reprogramming factors	Risk of insertional mutagenesis; potential for tumorigenesis; permanent genomic alteration
Lentiviral Transduction	Integrating	Can infect non-dividing cells; high efficiency; broader tropism	
Inducible Lentiviral Methods	Integrating	Temporal control over factor expression; reduced risk of insertional mutagenesis	Complex system; requires precise control and additional steps for transgene excision
Episomal Vectors	Non-Integrating	No genomic integration; extrachromosomal maintenance; reliable for certain cell types	Concerns about genetic integrity due to TP53 shRNA; lower efficiency compared to the integrating methods
Sendai Virus Reprogramming	Non-Integrating	Efficient; reliable; no genomic integration; low workload	Slow RNA clearance; dependence on one commercial supplier
Protein Reprogramming	Non-Integrating	Non-genetic approach; avoids genomic integration; eliminates risks of viral vectors	Lower efficiency; challenging protein synthesis
Small Molecules And Chemical Reprogramming	Non-Integrating	Low-risk reprogramming; controllable; reversible; avoids genetic modification	Lower efficiency
PiggyBac Transposon	Non-Integrating	Low-risk reprogramming; mobile genetic element	Risk of insertional mutagenesis; challenges in the excision process; potential for secondary transposition
Adenoviral Vectors	Non-Integrating	No genomic integration; can generate iPSCs from various cell types	Low transduction efficiency compared to retroviral vectors
Minicircle DNA	Non-Integrating	Efficient transgene expression; no genomic integration	Lower reprogramming efficiency; complex preparation
mRNA Transfection	Non-Integrating	No genomic signature; reduced immunogenic response; high efficiency	Requires daily transfections and specialized equipment
miRNA Reprogramming	Non-Integrating	No genomic integration; favorable safety profile; promising for clinical applications	Lower efficiency; requires precise delivery of small RNAs

### 2.6.3 Characterization of iPSCs

In order to ensure the quality, safety, and potential of iPSCs for clinical use, characterization must be undertaken. There is a wide range of molecular, functional, and phenotypic analyses that can be performed to confirm that iPSCs have, in fact, pluripotency features (Figure 2.2) [97], [98].

The first indicator of iPSC quality is their morphology, which resembles the morphology of ESCs. iPSCs are usually arranged in tightly packed colonies with smooth, defined borders. These cells are typically small, with a high nucleus-to-cytoplasm ratio. This appearance is characteristic of their pluripotent state, indicative of their ability for self-renewal and differentiation into a variety of cell types [97], [99].

In addition, the characterization of iPSCs consists of several other crucial elements.

Firstly, it is possible to perform molecular characterization, typically involving the identification of key pluripotency factors and proteins like NANOG, OCT4, SOX2, tumor-related antigens (TRA)-1-60/81, stage-specific embryonic antigens (SSEA)-3/4, and the expression of alkaline phosphatase (ALP). These markers are fundamental to assessing the pluripotent state of iPSCs [97], [98].

Secondly, to show the pluripotency of iPSCs, functional analyses are also conducted. In these tests, it is demonstrated that iPSCs have the ability to differentiate into cells of the three germ layers: ectoderm, endoderm, and mesoderm. This can be accomplished through *in vitro* analyses, including molecule-based differentiation or spontaneous embryoid body (EB) generation, or *in vivo* through the formation of a teratoma<sup>11</sup>. Consequently, the differentiation potential can be evaluated by the presence of certain markers characteristic of each germ layer. These include the Glial Fibrillary Acidic Protein (GFAP), the Neuroepithelial Stem Cell Protein (NESTIN), and the Paired Box Protein Pax-6 (PAX6) for ectoderm; Alpha Fetoprotein (AFP), Pancreatic and Duodenal Homeobox 1 (PDX1), Transcription Factor GATA-4 (GATA4) for endoderm; and Brachyury (TBXT), Vascular Endothelial Growth Factor receptor 1 gene (FLT1), Runt-related transcription factor 1 (RUNX1), and Forkhead Box Protein A2 (FOXA2) for mesoderm [97], [98].

Furthermore, it is necessary to evaluate the genomic stability and integrity of iPSCs to guarantee that there are no abnormalities that could have resulted from the reprogramming process. This involves monitoring for genotoxicity and the existence of residual reprogramming factors that could lead to tumorigenicity or other unfavorable outcomes [97].

In addition, the characterization process may also evaluate iPSC epigenetic status in order to ensure that they have undergone a complete reprogramming process and do not harbor any epigenetic memory of their somatic cell origin. This analysis is of the utmost importance, since incomplete reprogramming or the retention of somatic cell memory could impact both the differentiation potential and the applicability of iPSCs [97].

---

<sup>11</sup>Teratoma: A particular type of germ cell tumor that has the ability to contain several different types of tissue and may be mature or immature (they can occasionally contain both mature and immature cells). Teratomas may be benign or malignant [100].

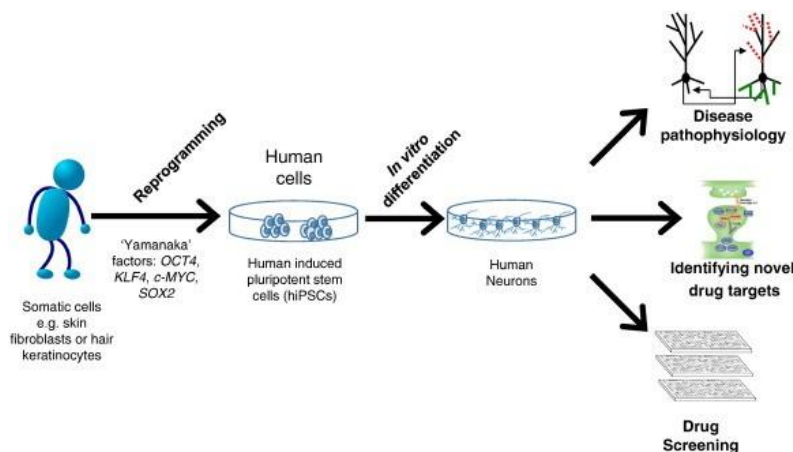


Figure 2.2: Schematic representation of the iPSC generation process [5].

#### 2.6.4 Neural Differentiation

Neural differentiation is a complex process that involves the transformation of pluripotent stem cells into specific types of neurons, including MNs [101]. It is a critical process in the development of the central nervous system (CNS) and can be essential for modeling neurodegenerative diseases [102].

There have been significant developments in the field of neural differentiation involving human Pluripotent Stem Cells (hPSCs), which collectively include ESCs and iPSCs. In recent years, a scalable and automated method has been developed to convert hPSCs into different neuronal subtypes. This procedure generates spinal and cranial MNs, spinal interneurons, and sensory neurons by systematically testing the combinatorial actions of small molecules on hPSCs [103].

The key to this approach's success is the ability to precisely regulate developmental cues such as Wingless-related integration site (*Wnt*), Fibroblast Growth Factor (*FGF*), Retinoic Acid (*RA*), and *Sonic Hedgehog* (*SHH*) signaling pathways, which are crucial for determining cell fate during embryonic development. This method promotes the differentiation process and enhances the efficacy of generating targeted cell types. In particular, the critical role of canonical *Wnt* signaling in specifying motor neuron variety was revealed, with graded *Wnt* signaling being essential for the generation of spinal or cranial motor neuron progenitors. In fact, in only 14 days, it is possible to achieve 74% efficiency in spinal motor neuron production and 52% efficiency in cranial motor neuron production. These neurons show characteristic molecular markers and functional features, including neurotransmitter response and action potential firing [103].

In addition to this approach, a different method has been introduced, which involves the dual inhibition of Suppressor of Mothers Against Decapentaplegic (SMAD) signaling, promoting rapid and complete neural conversion of over 80% of iPSCs under adherent culture conditions into Neural Stem Cells (NSCs) [104].

Following this, NSCs can be directed towards specific neuronal subtypes through a process known as "patterning", in which the development of the dorsal-ventral and the anterior-posterior axes of the neural tube is controlled by the use of morphogens or agonists/antagonists of specific signaling pathways involved. As a result of this dual inhibition method, neural induction efficiency is increased, which is demonstrated by the expression of the neuroectodermal marker PAX6. Furthermore, the initial cell density affects the ratio of central nervous system and neural crest progeny, making it possible to use iPSCs in disease modeling and

regenerative medicine without the need for stromal feeders or embryoid bodies [104].

Neural Crest Cells (NCCs) are generated from iPSCs and differentiate into peripheral neurons, glia, and non-neural cell types, which are the components of the peripheral nervous system [102], [105].

In addition, the differentiation of glial cells, such as astrocytes and oligodendrocytes, is also important. Astrocyte induction can be achieved using factors including Bone Morphogenic Protein (*BMP*), Ciliary Neurotrophic Factor (*CNTF*), basic Fibroblast Growth Factor (*bFGF*), and fetal bovine serum or serum-free medium with activin A, heregulin 1 $\beta$ , and Insulin-like Growth Factor 1 (*IGF-1*). On the other hand, the differentiation of oligodendrocytes requires several steps and prolonged growth factor administration [102].

### 2.6.5 Advantages of iPSCs compared to animal models

There are several advantages to iPSC use when compared to animal models. In the first place, these cells can be cultured in a carefully controlled laboratory environment, which allows the precise manipulation of variables and conditions. Secondly, they enable the study of individual cell or tissue processes in isolation, providing a comprehensive understanding of particular aspects of diseases. Furthermore, iPSCs offer a continuing cell source for experimentation because they are relatively easy to expand and maintain in culture. In addition, as they are a simplified model, iPSC use decreases the number of variables that could affect experimental outcomes, thereby simplifying result interpretation. Finally, using iPSCs reduces the demand for animal models, making them both cost-effective and ethically preferable [106].

### 2.6.6 Limitations of iPSC

iPSCs are an invaluable tool for improving our knowledge and treatment of ALS. However, as mentioned in Section 2.5, there are some limitations associated with the use of these cells. Variability between cell lines, which may be a result of reprogramming-induced genetic and epigenetic changes, can compromise the accuracy of disease models [107]. In addition, age-related characteristics are eliminated during the reprogramming process, resulting in a rejuvenated, embryonic state, which can limit the accurate study of late-onset diseases such as ALS [108], [109]. There have been attempts to induce aging *in vitro*. However, not only are they still in development, they have also not fully addressed this problem yet [105]. Furthermore, another limitation is the effectiveness and maturity of differentiated cells. The differentiation process can be inefficient, and it can take a long period of time to generate mature and functional cells ([105], [108]). Additionally, the epigenetic memory that iPSCs often retain from their cells of origin may limit their ability to properly differentiate into the target cell type and affect disease models' reliability [110].

The absence of standardized quality control and variation in experimental protocols also limit the use of iPSCs in ALS research. Variations in experimental results may arise from the variability of reprogramming methods, culture conditions, and donor cells' genetic background [107], [110]. Additionally, the genetic and epigenetic instability of certain iPSC lines may cause undesirable cell phenotypes, such as possible oncogenic changes [110].

In summary, although iPSCs present potential for modeling ALS and creating therapeutic approaches, there are still several challenges to overcome, including the variability and instability of iPSC lines [110], the inefficiency of differentiation [105], [108], the loss of age-related features [108], [109], and the absence of standardized protocols [107], [110]. Consequently, in order to fully use iPSCs for ALS research and therapy, these limitations must be addressed [110].

### 2.6.7 iPSCs Applications

As previously mentioned, iPSCs are a fundamental tool in regenerative medicine, drug discovery, and biomedical research. They are a viable alternative to embryonic stem cells as they enable the reprogramming of adult somatic cells to reprogram into pluripotent states without ethical and immunological limitations [93]. Therefore, iPSCs have several applications that will be discussed in further detail.

**Disease Modeling and Drug Discovery** iPSCs represent a powerful tool in disease modeling, as the generation of patient-specific iPSCs and their subsequent differentiation make it possible to mimic real disease states *in vitro*. This has been particularly useful in the study of neurodegenerative diseases, cardiovascular conditions, and genetic disorders. Furthermore, high-throughput drug screening and toxicity testing have been enhanced by the use of iPSCs, greatly improving the success of the drug development process [93].

**Regenerative Medicine and Cell Therapy** As a result of their ability to differentiate into numerous cell types, iPSCs have great potential in regenerative medicine and cell therapy. In fact, this potential has been employed in several clinical trials, including age-related macular degeneration, Parkinson's disease, and myocardial ischemia studies. Furthermore, iPSCs can also be used in autologous transplantation, which consists of reprogramming the patient's own cells into the necessary cell types, thereby reducing the risk of immunological rejection [93].

**Gene Editing and Personalized Medicine** Another use of iPSCs consists of the combination of two techniques: iPSCs and CRISPR/Cas9 gene editing technology<sup>12</sup>. This merge allows precise gene modification, correcting mutations that cause diseases, such as beta-thalassemia and hemophilia A. Additionally, the capacity to generate patient-specific iPSCs contributes to the creation of personalized treatments. As a result, therapies can be adjusted to individual genetic profiles, increasing therapeutic efficiency and minimizing adverse effects [112], [113].

**Three-Dimensional Organoids and Infertility Treatment** Recent developments have allowed the generation of three-dimensional organoids from iPSCs, mimicking the structure and function of human organs. There have been multiple organoids developed, including the stomach, gut, liver, lung, brain, and eye, offering a more physiologically accurate model for human development, disease, and drug response studies [113]. Furthermore, iPSCs have demonstrated infertility treatment potential by differentiating into male germ cells and producing functional spermatozoa [93].

**Veterinary Science and Conservation** Finally, iPSCs can also be used in veterinary research to validate stem cell therapies and assisted reproduction technologies in pre-clinical settings. Therefore, iPSCs are a promising tool in cloning efficiency enhancement and in the conservation of endangered species by offering a consistent supply of pluripotent cells for a variety of applications [93].

---

<sup>12</sup>CRISPR/Cas9 gene editing technology: Clustered regularly interspaced palindromic repeats is a gene-editing tool that allows the correction of genome errors and the turn on/off of genes in a fast, inexpensive, and relatively effortless way. It has several laboratory applications, such as the rapid generation of cellular and animal models, functional genomic screens, and live imaging of the cellular genome [111].

### 2.6.8 iPSCs as a Disease Model and Drug Screening tool

As referred to in Section 2.6.7, iPSCs are essential in disease modeling and drug screening, especially with neurological disorders. These cells are derived from patients with specific genetic pathologies, allowing for the creation of *in vitro* models that closely resemble this condition (patient-specific models). This ability is particularly important for dealing with the substantial burden of neurological diseases, for which there are currently few effective therapies and a low success rate for new compounds in clinical trials, mostly due to the lack of pertinent pre-clinical models [114].

iPSCs are also crucial in high-content screening, where a wide database of compounds is examined for possible therapeutic effects. In spite of having several technical challenges, such as the requirement for automation and sophisticated analysis systems, it holds great promise for discovering novel treatments for neurological disorders [114].

Furthermore, since iPSCs are able to identify subgroups of responders and nonresponders to specific treatments, they offer a unique possibility for precision medicine. This can result in more targeted clinical trial designs and better patient outcomes [114].

Blood-brain barrier (BBB) models derived from iPSCs have proven invaluable in the study of neurodegenerative diseases, providing a better understanding of the molecular and cellular mechanisms involved. These models can be used for drug screening in order to identify compounds that are able to restore the functions of the BBB or stabilize vascular structures, possibly preventing or slowing disease progression [115].

### 2.6.9 iPSCs use in ALS

The study of ALS (a neurodegenerative disease characterized by increasing motor neuron loss) has been transformed by the use of iPSCs [116]. The reprogramming procedure of somatic cells into iPSCs enables the differentiation of these into MNs, promoting the development of disease models and drug screening protocols [117].

Disease modeling is one of the main applications of iPSCs in ALS research. The differentiation of iPSCs (derived from ALS patients) into MNs allows for the creation of *in vitro* models that enable the study of ALS-related pathological pathways such as neurofilament aggregation, neurite degeneration, and TDP-43 proteinopathy (Section 2.4.1). As a result, these models enable the investigation of the underlying causes of disease and the identification of specific cellular changes involved in the development and progression of ALS [118].

Furthermore, iPSCs are favorable for genetic manipulation, allowing the correction of disease-causing mutations. This ability has been explored in other neurodegenerative diseases, and it may be used in the context of ALS to study the impact of correcting mutations in genes such as *SOD1*, *TARDBP*, and *C9ORF72* [118]. Through the comparison of MNs with and without these mutations, it is possible to further understand the molecular mechanisms responsible for ALS [117].

Additionally, iPSCs can be a powerful tool in the context of drug screening. iPSC-based models enable the investigation of the efficacy of potential therapeutics in a cellular setting that resembles the human condition. Through this approach, several compounds that decrease neuronal hyperexcitability [119] and modulate pathways, such as mTOR-autophagy and cytokine secretion, have been discovered, including Src/c-Abl inhibitors [116], [117]. These compounds have demonstrated potential for tackling ALS motor neuron degeneration [117].

iPSCs have also been used to study the role of astrocytes in ALS pathology. It has been demonstrated that ALS patients' iPSC-derived astrocytes contribute to non-cell autonomous effects on MNs, such as

autophagy mechanism impairment and enhanced toxicity, emphasizing the role of astrocytes in ALS and their potential as therapeutic targets [118].

In order to better mimic the *in vivo* environment, there has been an increasing interest in the development and use of 3D models, instead of the traditional 2D cultures. These models are able to advance our knowledge of ALS pathophysiology by offering insights into the interactions between various cell types and the extracellular matrix [118].

Another application of iPSCs in ALS is the development of patient-specific models that can be used to customize treatment plans based on individual genetic backgrounds. As discussed in Section 2.6.8, this method enables the identification of subgroups of responders and nonresponders to a particular treatment, potentially resulting in more specialized and efficient therapies [118].

Finally, sizable repositories of iPSC-derived cells from ALS patients (both familial and sporadic cases) have been developed in order to facilitate the identification of new therapeutic targets and possible candidates for clinical trials. As a result, through the analysis of the heterogeneity of ALS cases, models that better represent the clinical characteristics of the disease can be developed, including its sporadic forms [119].

## 3 Materials and Methods

### 3.1 Induced Pluripotent Stem Cells: cell lines used and their maintenance

In this study, four different cell lines were used: one from a healthy patient and three from ALS patients. Table A.1 (Appendix) contains information regarding these cell lines.

Induced Pluripotent Stem Cells (iPSCs) were cultured in *TeSR<sup>TM</sup>-E8<sup>TM</sup>* medium (StemCell Technologies®) in 35mm *Geltrex*-coated dishes (Gibco®). Generally, they were detached every 4-5 days using 1mg/mL of *Dispase II* (Roche®) in the presence of 10  $\mu$ M *Rock Inhibitor* (Selleckchem®).

During the maintenance phase, the main focus is the preservation of bigger cell clusters while excluding smaller colonies and single cells. Therefore, before the detachment, it is important to clean the colonies using a tip. This cleaning procedure is crucial because individual cells and small clusters with different morphologies could start to differentiate into different cellular lines, which could lead to the loss of pluripotency in the colonies. In addition, the exclusive preference for preserving larger, more uniform clusters is intended to produce a more controlled and consistent differentiation outcome.

### 3.2 *Geltrex* Matrix

iPSCs are grown on a fundamental matrix called *Geltrex*, which serves as an essential substrate for the cells' attachment to the culture dish. Different environmental circumstances cause specific changes in *Geltrex*'s physical state:

- Frozen Stage: *Geltrex* is kept in the freezer to preserve its rigid composition when it is in its solid condition.
- Liquid Stage: in this stage, *Geltrex* becomes liquid, allowing for the possibility of being diluted as needed.
- Gel-like Stage: during this stage, *Geltrex* is placed in the incubator (37°C) and undergoes a significant change, taking on a gel-like consistency that is essential in providing a supportive environment for iPSC adherence and expansion.

#### 3.2.1 *Geltrex* Preparation

Two days before the detachment procedure, the *Geltrex* aliquots are taken out of the -80°C freezer and placed in an ice bucket in the refrigerator at 4°C. This initial step serves to facilitate the transition of *Geltrex* from its frozen state to its liquid state.

On the next day, Geltrex is carefully diluted in *DMEM:F12* (*Dulbeco's Modified Eagle's Medium/Nutrient Mixture F12*), and the resulting solution is then uniformly dispensed in the designated wells or dishes. These dishes are then refrigerated at 4°C overnight, which enables the optimal integration of *Geltrex* into the culture environment.

On the day of detachment, the *Geltrex* dishes are transferred to the incubator at 37°C for at least 40 minutes before use. This specific time range is crucial because it guarantees that *Geltrex* will acquire a gel-like consistency. This period of time is essential and cannot be shortened.

Throughout the entirety of this process, the culture dishes are placed on a tray on top of a bucket of ice in order to keep a constant cold temperature (so that *Geltrex* remains liquid).

It is important to note that, before being placed in an overnight refrigerator at 4°C, the dishes should be shaken gently to uniformly distribute *Geltrex*. After this, the dishes are wrapped in *Parafilm®M* to prevent any kind of contamination.

A *Geltrex*-coated dish that is ready to use can be stored at 4°C for up to 15 days.

### 3.3 Detachment, splitting, and freezing procedures

The previously prepared *Geltrex* dishes are placed in the incubator around 40 minutes prior to the start time (minimum time). Subsequently, the old medium is removed from the dishes. The next steps consist of a thorough cleaning procedure, beginning with a 1 mL *DMEM:F12* rinse to successfully remove cell debris. The dish is gently shaken in order to promote the flotation of debris in the medium, and then the *DMEM:F12* is carefully aspirated and thrown away to guarantee a complete removal.

After that, a 500-µL wash with 1 mg/mL of *Dispase II* is carried out to remove any remaining *DMEM:F12* that could interfere with the enzymatic activity. After giving the dish a brief shake, the *Dispase II* is aspirated, and 1 mL is added for a 4-minute incubation period at room temperature, maintaining the procedure under the laminar flow hood. Following the incubation period, *Dispase II* is taken out, and one more wash using 1 mL of *DMEM:F12* is performed.

After aspirating the *DMEM:F12*, 1 mL is added to the dish. Using a cell scraper (Corning®), the cells are carefully detached from the dish by moving around its edge. After that, the cell suspension is transferred into a 15-mL tube.

An extra 1 mL of *DMEM:F12* is added to the dish, and the procedure is repeated if needed to guarantee the recovery of all colonies. The cell suspension is centrifuged for 4 minutes at room temperature and 1000 rpm. Then, the supernatant is carefully aspirated away without disturbing the pellet, the tube is gently flicked with the fingertip, and 1 mL of *TeSR™-E8™* medium with 10 µM *Rock Inhibitor* is added. Meanwhile, the *Geltrex*-coated dishes are retrieved from the incubator, and the old *DMEM:F12* is removed. The colony suspension is gently pipetted to guarantee uniform colony disruption.

After this, it is time for the splitting procedure. The splitting ratio depends on cell confluency.

When putting the dishes in the incubator, it is advisable to make a gentle cross-like movement. This procedure aims at distributing the colonies homogeneously over the dish, reducing the possibility of the formation of a concentrated colony in the center of the dish. If this problem is not addressed, it may lead to undesirable differentiation outcomes, particularly during the maintenance phase of the cell culture protocol.

The morning after splitting, the *TeSR™-E8™* medium with *Rock Inhibitor* is replaced with the *TeSR™-E8™* medium without *Rock Inhibitor*.

If cryopreservation is employed, 1 mL of *CryoStor*<sup>®</sup>*CS10* (StemCell Technologies<sup>®</sup>) is added to the 15 mL tube containing the pellet. After this, 1 mL of *CryoStor*<sup>®</sup>*CS10* is transferred into the 15 mL tube (for a total of 2 mL). The solution is then divided into two vials, placed on ice, and stored in a -80°C freezer. The vials are moved to a liquid nitrogen tank at -196°C for long-term storage after a minimum of 48 hours.

### 3.4 Motor neuron differentiation protocol

This protocol implements a combination of small molecules in a chemically defined neural medium to convert iPSCs into a near-pure population of Motor Neuron Precursors (MNP) within 24 days, followed by the generation of a highly enriched population of functional Motor Neurons (MN) over an additional 16-day period. Each phase of the differentiation protocol has a specific medium. All of these media share a common part that is the same for all of the formulations used in the different phases of the experimental protocol.

Table 3.1 presents the common constituents of the media, including their *Final Concentration*, *Stock Concentration*, *Dilution Factor*, and *Manufacturer*.

Table 3.1: Common constituents of all medium formulations.

Component	Final Concentration	Stock Concentration	Manufacturer
DMEM:F12 Medium	1X	-	Gibco <sup>®</sup>
Neurobasal Medium	1X	-	Gibco <sup>®</sup>
N2 Supplement	0.5X	100X	Gibco <sup>®</sup>
B27 Supplement	0.5X	50X	Gibco <sup>®</sup>
Ascorbic Acid	0.1 mM	10 mM	Santa Cruz <sup>®</sup>
Glutamax	1X	200 mM	Gibco <sup>®</sup>
Antibiotic Antimycotic Solution	1X	100 mM	Euroclone <sup>®</sup>

The remaining components of these media are phase-specific and are responsible for obtaining Neuroepithelial Progenitors (NEP), Motor Neuron Motor Neuron Precursors (MNP), Motor Neurons (MN), and mature MNs.

Tables 3.2, 3.3, 3.4, and 3.5 provide a list of the specific components of Media A, B, C, and D, respectively, which are added to the common medium detailed in Table 3.1.

Once confluency is reached, iPSCs are dissociated with *Dispase II*, as previously described in Section 3.3. Following that, a 1:6 cell split onto 35-mm-diameter *Geltrex*-coated plates is conducted in *TeSR*<sup>TM</sup>-*E8*<sup>TM</sup> medium with 10  $\mu$ M *Rock Inhibitor*. The next day, the original medium must be replaced with chemically defined neuronal Medium A. Before changing the medium, a wash with *DMEM:F12 medium* must be done in order to completely remove the *TeSR*<sup>TM</sup>-*E8*<sup>TM</sup> medium with *Rock Inhibitor*.

Table 3.2: Medium A formulation.

Component	Final Concentration	Stock Concentration	Manufacturer
Common Medium	-	-	-
CHIR 99021	3 $\mu$ M	10 mM	Tocris <sup>®</sup>
DMH-1	2 $\mu$ M	10 mM	Tocris <sup>®</sup>
SB431542	2 $\mu$ M	10 mM	Stemgent <sup>®</sup>

Throughout the progression of this induction stage, a medium change is applied on different days, namely at Time (day) 0, 2, 4, 6, and 8. The goal is to have a population of NEPs that exhibit immunopositivity for the transcription factor *SOX1* by the end of this phase.

*Dispase II* (1 mg/mL) should be administered to help in the dissociation of NEP cells. Afterwards, a 1:6 cell split is executed onto *Geltrex*-coated plates. The cells are subsequently supported in their continuous growth and differentiation by the introduction of Medium B, the culture medium for this stage.

Table 3.3: Medium B formulation.

Component	Final Concentration	Stock Concentration	Manufacturer
Common Medium	-	-	-
CHIR 99021	1 $\mu$ M	10 mM	Tocris®
DMH-1	2 $\mu$ M	10 mM	Tocris®
SB431542	2 $\mu$ M	10 mM	Stemgent®
Retinoic Acid	0.1 $\mu$ M	1 mM	Stemgent®
Purmorphamine	0.5 $\mu$ M	1 mM	Stemgent®

It should be noted that obtaining a sufficient number of NEP cells is necessary before beginning the splitting process. The degree of confluency must be determined before starting this passage. In circumstances where the cell density is insufficient, a more successful strategy involves merging cells from two or more dishes before performing a 1:6 split onto *Geltrex*-coated dishes.

A schedule where the culture medium is replaced every other day is established, namely at Time (day) 0, 2, 4, and 6 during the progression of this stage. At the end of this phase, the aim is to have a population of MNPs with immunopositivity for the *OLIG2* transcription factor.

*Dispase II* (1 mg/mL) should be used to dissociate *OLIG2*<sup>+</sup> MNPs on *Geltrex*-coated plates. Next, a 1:20 cell split is begun along with the addition of the designated culture Medium C in order to sustain the cells' continued development.

Table 3.4: Medium C formulation.

Component	Final Concentration	Stock Concentration	Manufacturer
Common Medium	-	-	-
Retinoic Acid	0.5 $\mu$ M	1 mM	Stemgent®
Purmorphamine	0.1 $\mu$ M	1 mM	Stemgent®

It is important to mention that it is imperative to attain a substantial cell population while guaranteeing the presence of empty space to promote the formation of complex cell networks.

As this stage progresses, the routine of altering the culture medium every other day at Time (day) 0, 2, 4, and 6 is established. At the end of this phase, the aim is to have a population of MNs that are immunopositive for the markers *MNX1* (*HB9*), *ISL-1*,  *$\beta$ TUB*, and *MAP2*.

The dissociation of *MNX1*<sup>+</sup> MNs is performed at the end of this stage using *Accumax*<sup>TM</sup> (StemCell Technologies®). In this case, after the removal of the old medium, a 1 mL DPBS rinse is done to efficiently remove cell debris. The dish is gently shaken in order to promote the fluctuation of debris in the medium, after which the DPBS is carefully aspirated and discarded to ensure a complete removal. After this, 1 mL of *Accumax* is added to promote cell detachment from the dish, and then the dish is placed in the incubator for 5 minutes. Meanwhile, two falcon tubes with 1 mL of Medium D in each are prepared. Once the incubation period ends, the dishes are placed again under the laminar flow hood, and the *Accumax* solution containing the detached cells is carefully aspirated, capturing only the floating cells, and transferred to one of the falcon tubes that had already been prepared. Subsequently, 1 mL of Medium D is added to the falcon tube, ensuring that the volume is twice as large as the *Accumax* in order to neutralize it. Following this, the cells are centrifuged using the same settings as in other detachment procedures. After centrifugation, the supernatant is carefully aspirated without disturbing the pellet. The tube is gently flicked with the fingertip, after which 1 mL of Medium D is added in order to resuspend the cell solution. In this phase, the size of the pellet must be evaluated in order to determine the appropriate dilution factor (if the pellet is substantial, a higher dilution factor must be considered). After completing the dilution in the second falcon tube, 10  $\mu$ L of the cell solution are placed in a chamber of the cell-counting chamber device (Figure 3.1). Three chambers must be loaded for analysis. Under the microscope, the cells in each chamber are counted with the aid of a cell counter device (Figure 3.2), and an average count is then calculated. Cells were seeded at a density of 100 000 cells per well in a 24-multiwell plate with *Geltrex*-coated glass coverslips. In the end, each well should have a total volume of 500  $\mu$ L of Medium D.

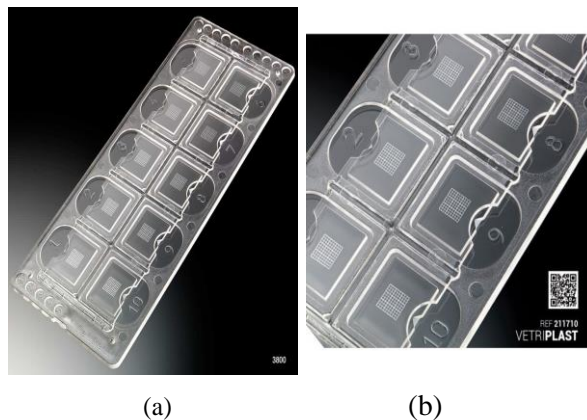


Figure 3.1: a) Cell-counting chamber device; b) Chamber of a cell-counting chamber device.



Figure 3.2: 1-key manual cell counter device.

Twenty-four hours after seeding the cells, a new Medium D is prepared, only enriching it with trophic growth factors including *Brain-Derived Neurotrophic Factor (BDNF)*, *Insulin-Like Growth Factor 1 (IGF-1)*, and *Ciliary Neurotrophic Factor (CNTF)* at a final concentration of 10 ng/mL for each to induce MN maturation. Finally, the medium is replaced every three days for a duration of 10 to 12 days.

At the conclusion of this phase, the goal is to obtain a population of mature MNs that express *Choline Acetyltransferase (ChAT)* is the most specific marker for cholinergic neurons).

Table 3.5: Medium D formulation.

Common Medium	Final Concentration	Stock Concentration	Manufacturer
Common Medium	-	-	-
Retinoic Acid	0.5 $\mu$ M	1mM	Stemgent®
Purmorphamine	0.1 $\mu$ M	1mM	Stemgent®
Compound E	0.1 $\mu$ M	1mM	StemCell Technologies®

### 3.5 Immunocytochemistry

At the end of each phase of the differentiation protocol, the cells are placed on a coverslip inside a well of a 24-multiwell plate, pre-coated with *Geltrex*.

An immunocytochemistry experiment is performed in order to evaluate the presence of specific markers indicative of each differentiation phase. Specialized antibodies that can identify and bind to these markers are used in this experiment (Table A.2, Appendix). The results obtained from this procedure provide useful information about the cellular characteristics and marker expression at the conclusion of the corresponding phase.

#### 3.5.1 Protocol

One or two days after seeding, the following procedure is carried out:

1. The old medium is aspirated, and PBS 1X (pH 7.4) is gently added to each well. A 5-minute incubation period is undertaken.
2. Once the incubation period is over, the solution is slowly removed from each well.
3. Another 5-minute wash with *PBS 1X* is conducted.
4. After this, *PFA* (4%) is added to each well, and a 20-minute incubation period is undertaken. Subsequently, the solution is carefully removed from the wells.
5. Subsequently, the wells are washed again with *PBS 1X*, and a 5-minute incubation period is carried out.

After the incubation period, if the experiment cannot be continued on that day, the *PBS 1X* solution is removed from the wells and a medium containing *PBS* + 0.06% *NaN<sub>3</sub>* (sodium azide) is added. The addition of sodium azide serves as a conservative, allowing the cells to be stored in the refrigerator (4°C) for a longer period of time without experiencing any changes.

6. After step number 5, the coverslips are placed in the immunocytochemistry device (Figure 3.3) using a clamp and a hook.
7. A permeabilization solution (*PBS 1X* + 0.25% *Triton X-100* (*Tx*, Sigma®)) is added to each coverslip, followed by a 5-minute incubation period.
8. Subsequently, the blocking solution must be prepared.

Therefore, it is necessary to consider the information from Table A.2 (Appendix) in order to choose the appropriate blocking solution to use. The composition of the blocking solution involves *PBS 1X*, *Triton X-100* (*Tx*), and normal serum; the latter varies according to the secondary antibody used.



Figure 3.3: Device used to place the coverslips during the immunocytochemistry experiment.

9. After step number 8, the blocking solution is added to each coverslip, starting a 1-hour incubation period.
10. Subsequently, the primary antibody solution is added to each coverslip, initiating the overnight incubation period. Before being refrigerated, the immunocytochemistry device (Figure 3.3) must be filled with water. This prevents coverslips from drying overnight, as water-induced condensation helps to maintain a suitable environment.
11. The next morning, three washes with *PBSIX* are carried out, with a 5-minute incubation period after each wash.
12. In the meantime, it is necessary to centrifuge the vial containing the secondary antibody and the fluorochrome. It is crucial to complete this procedure to ensure the proper settling of any unbound portions of the fluorochrome. If this procedure is not completed successfully, it could result in signal interference when observing the sample under the microscope.
13. After Step 11, each receives the secondary antibody solution. This initiates a 2-hour incubation period. The device should remain closed throughout this period of time since the fluorochrome is light-sensitive and needs to be protected from light exposure.
14. After the 2-hour incubation time, the *Hoechst 33342* (10 mg/mL) solution is added to each coverslip, followed by an incubation period of 15 minutes. The application of this solution allows the staining of the cell nuclei.
15. After Step 14, it is necessary to perform three 5-minute washes with *PBSIX*.
16. Finally, one drop of *Dako® Fluorescent Mounting Medium* is applied to the slide for each coverslip. Before placing the coverslips in the mounting medium, it is crucial to turn them to ensure that the cells are in contact with the medium.

### 3.6 Quantification and Morphological analysis of $\beta$ TUB-Positive Motor Neurons

The morphometric analysis of cells immunostained for  $\beta$ TUB was performed at DIV30. These images were acquired with a 20X objective using a *Leica DFC310 FX digital camera* mounted on a *Leica DM5000B fluorescence microscope* equipped with *Leica Application Suite Software* (version 3.8.0).

Ten fields per condition were acquired. The quantification of *Hoechst*<sup>+</sup> nuclei was performed using the software *ImageJ Fiji* (1.52n, Wayne Rasband, NIH, <http://imagej.nih.gov/ij>), and the length of all neurites in each  $\beta$ TUB<sup>+</sup> cell was measured using the *NeuronJ* plugin of the *ImageJ Fiji* software.

The total number of  $\beta$ TUB<sup>+</sup>/*Hoechst*<sup>+</sup> nuclei was normalized to the total number of *Hoechst*<sup>+</sup> nuclei present in the analyzed fields in order to determine the percentage of differentiation, and the average neurite length relative to the total number of  $\beta$ TUB<sup>+</sup> cells was calculated for each condition.

### 3.7 Analysis of ChAT expression levels

In order to analyze *ChAT* expression levels, there are a number of procedures that must be performed. In the first place, RNA should be extracted from the samples. In the second place, reverse-transcription and cDNA synthesis should be carried out. Finally, *Reverse Transcription Polymerase Chain Reaction (RT-PCR)* should be performed, followed by the electrophoresis procedure.

#### 3.7.1 RNA extraction

MNs were seeded in six wells of a 24-multiwell plate at a density of 100 000 cells per well. At DIV40, the cells were collected for RNA extraction using the *ReliaPrep RNA Cell Miniprep System* (Promega®) extraction kit.

Extraction was carried out with the following steps:

1. The lysis buffer was supplemented with *tioglycerol* (10  $\mu$ L/mL of LB) and shaken. Cells were then lysed and subsequently homogenized using a syringe.
2. Isopropanol was added to the tube, and mixed by vortexing for about 5 seconds.
3. The sample was moved into a filtered column placed onto a collecting tube, and then centrifuged for 30 seconds at 12000 rpm, so that the RNA would bind to the filter.
4. The eluate was discarded and 500  $\mu$ L of *RNA Wash Solution (RWA)* were added to the tube, again centrifuging with the same settings of the last step. The eluate was discarded.

5. 3  $\mu\text{L}$  of *DNaseI* were suspended into 24  $\mu\text{L}$  of *Yellow Core Buffer* supplemented with 3  $\mu\text{L}$  of *MnCl<sub>2</sub>*, and the tube was gently shaken. 30  $\mu\text{L}$  of *DNaseI* mix were then added to the column directly on the filter, and the sample was incubated for 15 minutes.
6. 200  $\mu\text{L}$  of *Column Wash Solution (CWS)* were added to stop *DNaseI* activity, and the sample was centrifuged at 12000 RPM for 15 seconds.
7. Without discarding the eluate, 500  $\mu\text{L}$  of *RWA* were added and the sample was centrifuged at 12000 RPM for 30 seconds.
8. The column was moved onto a new tube and 300  $\mu\text{L}$  of *RWA* were added. The sample was centrifuged at 15000 RPM for 2 minutes, and then centrifuged again at 12000 RPM for 30 seconds.
9. The column was moved onto the collection tube and 30  $\mu\text{L}$  of *RNase-FREE water* was added directly onto the filter.
10. The sample was centrifuged at 12000 RPM for 1 minute. The eluate represented the extracted RNA.

The extracted RNA was then quantified using *Nanodrop-1000 Spectrophotometer* (ThermoScientific) and stored at  $-80^{\circ}\text{C}$ .

### **3.7.2 Reverse-transcription and DNA synthesis**

Reverse-transcription is a technique that employs the enzyme called *Reverse Transcriptase (RT)* to produce a cDNA molecule from an RNA template.

1  $\mu\text{g}$  of extracted RNA was reverse-transcribed using the *iScript cDNA Synthesis kit* (BIO-RAD). The reaction mix was composed of 4  $\mu\text{L}$  of *iScript Reaction Mix*, 1  $\mu\text{L}$  of *iScript reverse transcriptase*, 1  $\mu\text{g}$  of RNA and a variable amount of  $\text{H}_2\text{O}$  specifically provided by the kit to obtain an optimal volume (20  $\mu\text{L}$  total). The amount (in  $\mu\text{L}$ ) of RNA to add to the mix was calculated based on the RNA concentration resulted from the previous quantification.

When the mix was prepared, it was incubated into a *C1000 Thermal Cycler* (BIO-RAD), undergoing the following thermal cycles:

- 5 minutes at  $25^{\circ}\text{C}$
- 30 minutes at  $42^{\circ}\text{C}$
- 15 minutes at  $48^{\circ}\text{C}$
- 5 minutes at  $85^{\circ}\text{C}$
- maintenance at  $4^{\circ}\text{C}$

### 3.7.3 Reverse Transcription Polymerase Chain Reaction (RT-PCR)

RT-PCR is a technique used to estimate the presence of a gene in a population of cells, and it is based on the common Polymerase Chain Reaction (PCR), which employs the activity of DNA polymerase to selectively amplify a specific DNA fragment using a pair of primers whose sequences are complementary to those flanking the DNA of interest. However, whereas PCR is performed on extracted DNA, RT-PCR is performed on cDNA obtained through the reverse-transcription of extracted RNA.

In this study, RT-PCR was used to measure the levels of *CHAT* in the cell lines used.

Specifically, total RNA was extracted, and reverse-transcribed as previously explained. The cDNA was then used to perform a PCR.

The primers used are the following:

- *hCHAT*-Forward: 5' TGGCTTCCAACGAGGACGAG 3'
- *hCHAT*-Reverse: 5' GTCCCGGTTGGTGGAGTCTTT 3'

The reaction mix (25  $\mu$ L/well) was composed of:

- 0.4  $\mu$ M primers.
- 0.2 mM *dNTPs* (*dTTP*, *dGTP*, *JCTP*, *dATP*).
- Buffer 1x supplemented with *MgCl<sub>2</sub>*.
- *Taq DNA polymerase* (32 U/mL; VWR International).
- 1  $\mu$ L of cDNA.
- *H<sub>2</sub>O* to make up to volume.

Additionally, two different controls were used:

- Control sample (labeled as "0") containing all the reagents required for the amplification except the cDNA, to provide evidence of absence of contamination.
- *RT* sample containing all the reagents required for the reverse-transcription except the reverse transcriptase, to guarantee the absence of false positives (labeled as "-RT").

When prepared, the mix was incubated in a *Gene Amp PCR System 9700* (Applied Biosystems). The thermal cycling protocol involved the following steps, with steps 2, 3, and 4 undergoing 35 cycles:

1. 3 minutes at 95°C
2. 30 seconds at 95°C
3. 30 seconds at 60°C
4. 30 seconds at 72°C
5. 7 minutes at 72°C

### 3.7.4 Electrophoresis

Electrophoresis Agarose Gel is used to separate PCR products by size for visualization purposes. This technique employs an electrical field to move the negatively charged DNA towards a positive electrode through an agarose gel matrix. Moreover, shorter DNA fragments migrate through the gel matrix more quickly than the longer ones, and the DNA fragment can be identified by running it alongside a DNA ladder.

For the *ChAT* gene, a 2% (g/mL) agarose gel was prepared in a *TAE IX* buffer composed of:

- *Trizma Base* 0.04 M.
- *Acetic acid* 0.02 M.
- *EDTA* 1 mM.
- *Ethidium Bromide* 0.5  $\mu\text{g/mL}$  (SIGMA-ALDRICH).

*Ethidium Bromide* is an intercalating agent which can fit between bases into the double strands of DNA, emitting fluorescent light when irradiated with UV rays. DNA bands can thus be seen after migration.

### 3.8 Statistical Analysis

All results are reported as mean  $\pm$  standard deviation. Statistical comparisons between the ALS and NORM cell lines were conducted by applying a t-test. A p-value of less than 0.05 was set as significant. All statistical analysis were performed with the GraphPad Prism® software.

## 4 Results and Discussion

### 4.1 Generation and Evaluation of iPSC-derived ALS Motor Neurons

Given the significant challenges associated with obtaining primary cell types involved in neurodegenerative diseases (nervous system cells), the use and differentiation of iPSCs derived from patients with these pathologies offer a promising alternative. One of the advantages of using iPSCs is that they preserve the genetic information of the donor, enabling the reproduction of molecular events underlying the development of the disease in humans *in vitro*. Therefore, it represents a more accurate cellular model compared to the use of, for example, immortalized cells.

In this study, MNs were generated from three iPSC lines derived from patients affected by ALS using a protocol published in the literature [10], after some modifications.

The developmental stages that occur *in vivo* are followed by *in vitro* cellular differentiation. In the first place, there is a neural induction phase, followed by caudalization and ventralization [105]. This *in vitro* process is achieved through a combination of small molecules within a chemically defined neural culture medium.

The subsequent small molecules were used:

- **CHIR99021**, which is a promoter of the activation of the *WNT* signaling pathway, enhances neural induction, neuroepithelial proliferation, and stimulates neural progenitors towards a caudal fate;
- **SB431542**, which is an inhibitor of the TGF- $\beta$ /Activin/NODAL pathway, blocks the pluripotent state and promotes differentiation towards neuroectoderm;
- **DMH-1**, which is a BMP-mediated signaling inhibitor, favors the differentiation of iPSCs into neural precursors;
- **Retinoic Acid (RA)**, which is the derived form of Vitamin A, promotes neural differentiation and caudal identity;
- **Purmorphamine**, which is an agonist of *Shh*-mediated signaling, promotes ventralization.

Differentiation was also performed in parallel on a cell line from a healthy patient (30HU-002 (NORM)), used as control.

The cells were exposed to a medium containing CHIR99021, SB431542, and DMH-1 during the first 10 days of differentiation. This medium is responsible for "dual SMAD inhibition", allowing the inhibition of mesodermal and endodermal differentiation of iPSCs and promoting the development towards neuroectoderm by blocking the Activin/TGF $\beta$  and BMP signaling pathways, respectively. Thus, through a single chemically defined step that combines induction and caudalization phases, NEPs were obtained.

The induction of NEPs towards the MNP phenotype was achieved by exposing the cell culture to a medium containing RA and Purmorphamine throughout the following 7 days, in addition to the previously used molecules. This combination promotes ventralization of the culture.

Once MNPs were obtained, they were subjected to a medium with a higher concentration of RA and a lower concentration of Purmorphamine. These concentrations enhance the expression of crucial transcription factors necessary for the specification and differentiation of MNPs into MNs. After obtaining MNs, a maturation phase follows.

During the last phase of differentiation, the medium was supplemented with Compound E, an inhibitor of the NOTCH signaling pathway, to prevent the proliferation and differentiation of any residual precursors into other cell types. Compound E reduces the time of the maturation process, while also increasing the mature MN population. In order to promote further MN maturation, GFs were added to the medium, including BDNF, IGF-1, and CNTF.

Figure 4.1 shows the experimental timeline of the differentiation protocol. The stage-specific markers that must be identified in each phase can be seen below the timeline, while the time point at which the new medium of differentiation is introduced is shown above. It is also important to note that, even though the final phase begins at DIV24, the immunocytochemical staining is not conducted until the 30<sup>th</sup> day *in vitro* (DIV30), since staining is not possible before that time because the cells are not fully attached to the coverslips.

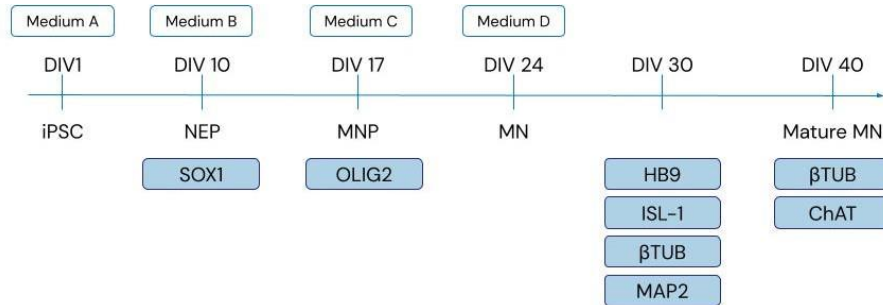


Figure 4.1: Schematic representation of the experimental timeline, indicating the respective markers to be identified in each phase.

In Figure 4.2, it is possible to observe iPSCs during the maintenance stage, which signifies the initial phase before the beginning of differentiation. In this stage, the cells remain undifferentiated and are arranged in large clusters. This distinctive appearance reflects their pluripotent nature and sets the stage for the subsequent differentiation process.

To maintain them in the pluripotent stage, the dishes should be cleaned to remove smaller clusters that can potentially differentiate into different cell types.

In this figure, cells from the 30HU-002 (NORM), the 30HU-004 (sALS), the CS52iALS-C9n6, and the Cs04iALS-SOD1H44Rn3 cell lines (A-D) can be observed, respectively.

The cells were maintained in culture until DIV40. During the differentiation process, it was possible to observe the morphological changes that the cells went through at each stage using a contrast-phase microscope. Figures 4.2, 4.3, 4.5, 4.7, and 4.10 show these morphological differences.

In Figure 4.3, it is possible to see cells at the end of the initial phase of differentiation. At this stage, they have transitioned from iPSCs to NEPs. These cells exhibit a notable transformation, adopting a more

elongated, neural-like appearance. Compared to iPSCs, there is a noticeable increase in cell density and organization within the culture. Additionally, the formation of rosette-like structures, characterized by round structures, is evident, signifying the development of NEPs.

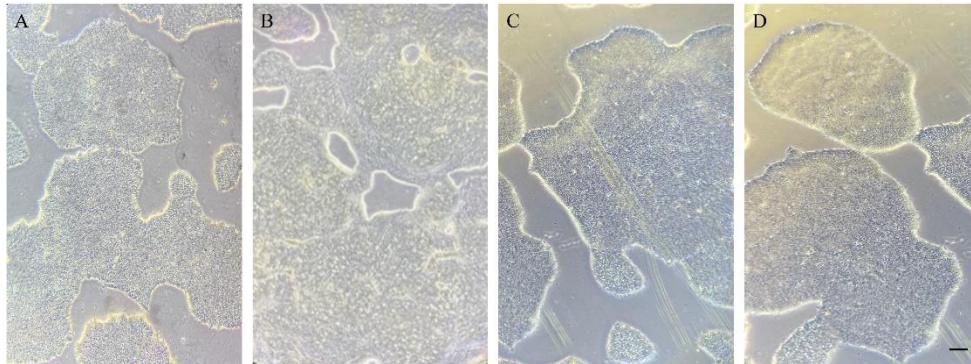


Figure 4.2: Bright Field (BF) images of iPSC colonies from four different cell lines in maintenance culture: (A) 30HU-002 (NORM), (B) 30HU-004 (sALS), (C) CS52iALS-C9n6, and (D) Cs04iALS-SOD1H44Rn3. Scale bar = 200 $\mu$ m

In this figure, it is possible to observe cells from the 30HU-002 (NORM), the 30HU-004 (sALS), the CS52iALS-C9n6, and the Cs04iALS-SOD1H44Rn3 cell lines, respectively (A-D).

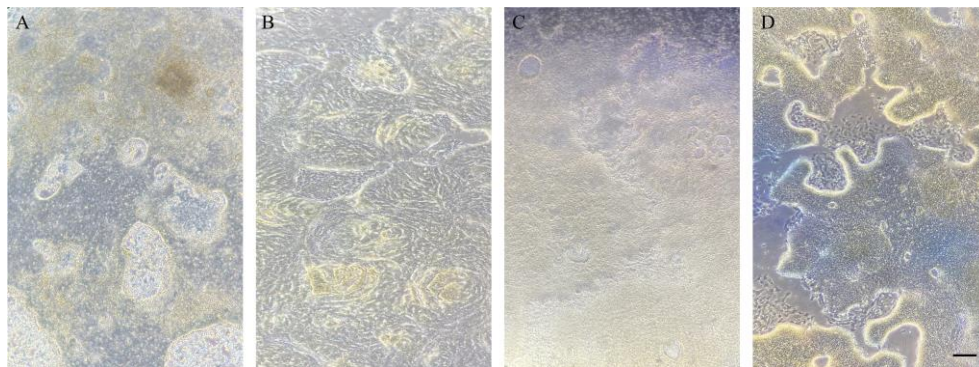


Figure 4.3: Bright Field (BF) images of iPSC colonies from four different cell lines in Medium A culture: (A) 30HU-002 (NORM), (B) 30HU-004 (sALS), (C) CS52iALS-C9n6, and (D) Cs04iALS-SOD1H44Rn3. Scale bar = 100 $\mu$ m

In order to further confirm that the desired cells were obtained at each stage of differentiation, the cells were plated in 24-multiwell plates with glass coverslips. These coverslips were then subjected to fluorescence immunostaining to assess whether the stage-specific markers of motoneuronal differentiation were present.

The first analysis at DIV10 was conducted to evaluate the presence of the nuclear marker SOX1 (Figure 4.4). SOX1 is a transcription factor and stands as the first and most specific marker for mammalian neural progenitors. It is expressed in NEPs, and assessing its expression helps to evaluate the effectiveness of the neural induction of the iPSC colonies. The primary and secondary antibodies used in this analysis are listed in Table A.2 (Appendix).

Additionally, *Hoechst* dye No. 33342 was used for nuclear staining in the different immunocytochemical

experiments.

As a transcription factor, SOX1 is primarily found within the nucleus of cells, regulating the expression of genes involved in neural development and differentiation. When observing SOX1's expression under the microscope, it is common to observe colocalization with *Hoechst* stain, a fluorescent dye that binds to the double strands of DNA. This colocalization indicates that SOX1 is present within the nucleus. The combination of SOX1 and *Hoechst* staining provides valuable insights into the localization and activity of this crucial transcription factor in the context of neural differentiation.

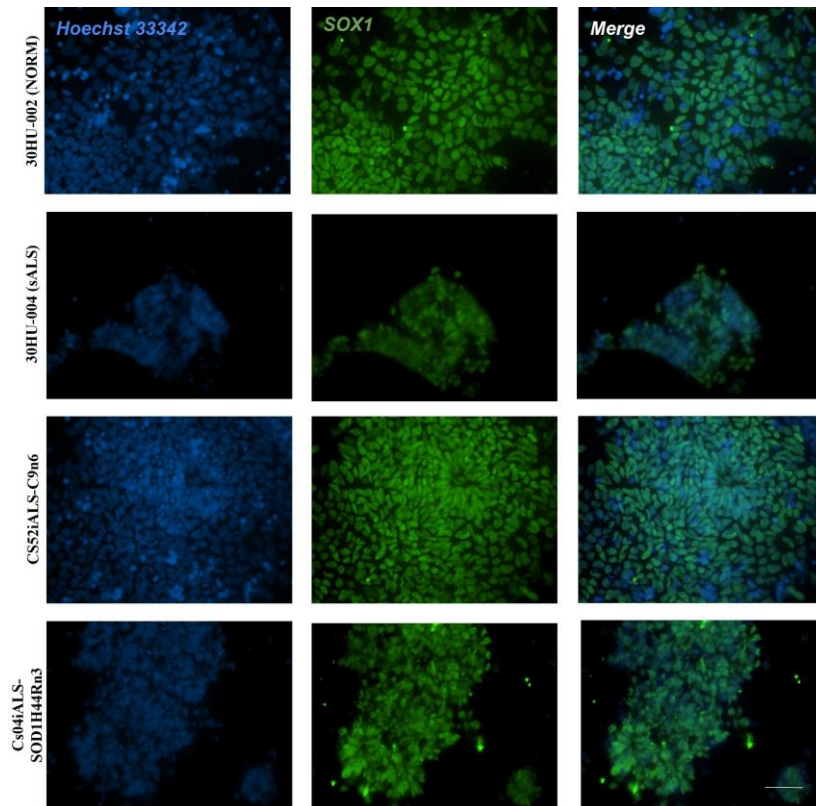


Figure 4.4: Immunocytochemical analysis of NEPs at DIV10, stained for the marker SOX1. The first row shows cells from the 30HU-002 (NORM) cell line, the second from the 30HU-004 (sALS) cell line, the third from the CS52iALS-C9n6 cell line, and the fourth from the 3Cs04iALS-SOD1H44Rn3 cell line. Scale bar = 50  $\mu$ m.

Figure 4.5 shows cells at the conclusion of the second phase of differentiation. At this stage, the cells have transitioned into MNPs. These cells present a distinct neuronal morphology, characterized by elongated cell bodies and the emergence of neurites resembling axons and dendrites. There is a noticeable increase in complexity and organization compared to previous stages, indicating the progression towards the motor neuron lineage.

In this figure, it is possible to observe cells from the 30HU-002 (NORM), the 30HU-004 (sALS), the CS52iALS-C9n6, and the Cs04iALS-SOD1H44Rn3 cell lines, respectively (A-D).

At the end of this phase, at DIV17, the expression of the OLIG2 marker was analyzed (Figure 4.6). OLIG2 is a *basic-helix-loop-helix (bHLH)* transcription factor that is essential to support the development

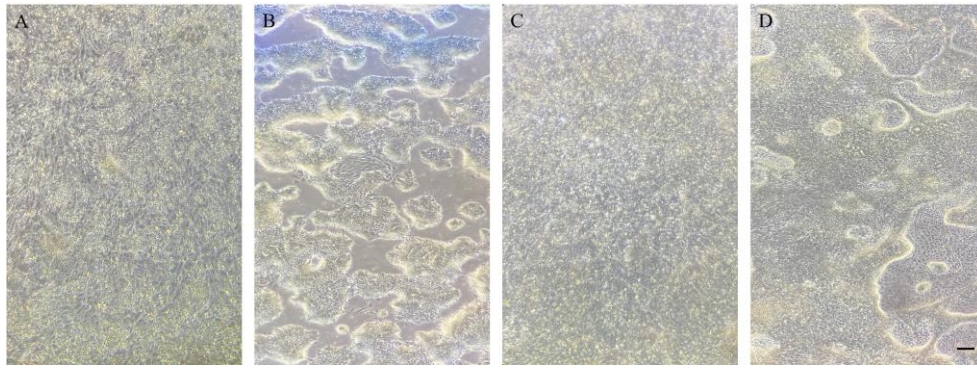


Figure 4.5: Bright Field (BF) images of iPSC colonies from four different cell lines in Medium B culture: (A) 30HU-002 (NORM), (B) 30HU-004 (sALS), (C) CS52iALS-C9n6, and (D) Cs04iALS-SOD1H44Rn3. Scale bar = 100 $\mu$ m

of the nervous system. It is crucial to determine the motor neuron and oligodendrocyte fates as well as to choose whether to proliferate or differentiate neural progenitors. The primary and secondary antibodies used in this analysis are listed in Table A.2 (Appendix).

As a transcription factor, OLIG2 is predominantly located within the nucleus of cells, where it plays a pivotal role in regulating the expression of genes involved in neural development and differentiation. When examining OLIG2 expression, it is common to observe colocalization with *Hoechst* stain, which serves as an indicator that OLIG2 is localized within the nucleus of cells. By combining OLIG2 and *Hoechst* staining, valuable insights into the localization and activity of this transcription factor within the context of neural differentiation are gained.

Figure 12 shows cells following the completion of the third phase of differentiation. At this stage, the cells have progressed into MNs. It is possible to observe elongated cells featuring a distinct cell body, from which multiple processes extend. These processes, referred to as neurites, encompass both axons and dendrites, imparting a distinctive bipolar morphology to the cell. This characteristic appearance is indicative of the MN's specialized structure and function in transmitting signals to muscle fibers and other neurons.

In this figure, it is possible to observe cells from the 30HU-002 (NORM), the 30HU-004 (sALS), the CS52iALS-C9n6, and the Cs04iALS-SOD1H44Rn3 cell lines, respectively (A-D).

Upon completing this phase, at DIV24, the expression of several markers was assessed (at DIV30). The first marker to be analyzed was HB9, a protein that is crucial in the postmitotic specification of spinal cord motor neurons (Figure 4.8). In addition to analyzing the expression of HB9, a second immunostaining was performed for another transcription factor, ISL-1. ISL-1 is a transcription factor in the LIM (LIN-11, Isl-1 and MEC-3) homeodomain essential for embryonic organ development, and it is necessary for the survival and specification of spinal cord motor neurons and cranial ganglia neurons. Besides, it is expressed in postmitotic motor neurons and contributes to cell body localization and axon development (Figure 4.9). Additionally, along with ISL-1, immunostaining for MAP2 was carried out. MAP2 is a protein that binds to microtubules and plays a critical role in the stabilization and organization of the microtubule network in cells. It is also essential for the development and maintenance of dendrites in neurons (Figure 4.9). Finally, the expression of the  $\beta$ TUBIII protein was analyzed.  $\beta$ TUBIII is a protein present in the microtubules, and it is crucial for several cellular functions, including intracellular transport and cell division.

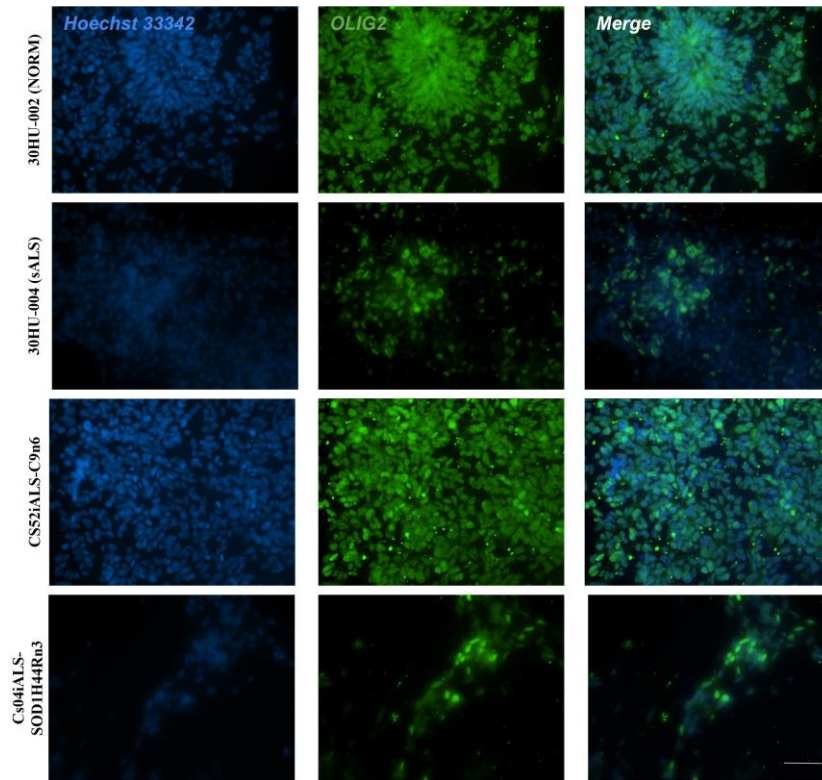


Figure 4.6: Immunocytochemical analysis of MNPs at DIV17, stained for the marker OLIG2. The first row shows cells from the 30HU-002 (NORM) cell line, the second from the 30HU-004 (sALS) cell line, the third from the CS52iALS-C9n6 cell line, and the fourth from the Cs04iALS-SOD1H44Rn3 cell line. Scale bar = 50  $\mu$ m.

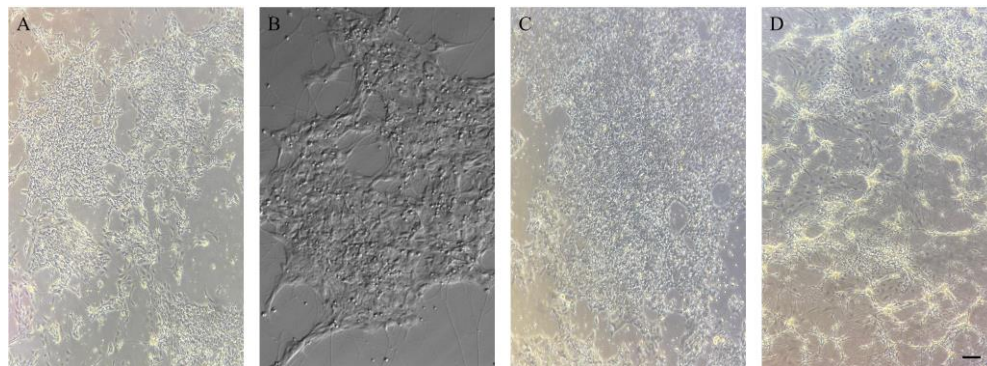


Figure 4.7: Bright Field (BF) images of iPSC colonies from four different cell lines in Medium C culture: (A) 30HU-002 (NORM), (B) 30HU-004 (sALS), (C) CS52iALS-C9n6, and (D) Cs04iALS-SOD1H44Rn3, respectively. Scale bar = 200  $\mu$ m

In MNs, it is found throughout the cell, in structures such as the soma, dendrites, and axons. The primary and secondary antibodies used in this analysis are listed in Table A.2 (Appendix).

As transcription factors, HB9 and ISL-1 can be found within the nucleus of the cells. When examining their expression, it is possible to observe colocalization with *Hoechst* stain, indicating the presence of these

markers within the cells' nucleus. The combination of HB9 and ISL-1 with *Hoechst* staining provides valuable insights into their localization and activity.

HB9 expression was found in all cell lines. However, the expression of HB9 in the Cs04iALS-SOD1H44Rn3 cell line was lower, and, by the combination with *Hoechst* staining, it is possible to observe that only some cells express this marker. This can be due to the intrinsic characteristics of the *SOD1* mutation. As HB9 is involved in maintaining MN identity and survival, low expression of HB9 in mutant *SOD1* patients may reflect motor neuron dysfunction, disease progression, impaired regeneration, and dysregulated gene expression.

MAP2 can be found in the dendrites of neuronal cells. By observing its expression in Figure 4.9, it is possible to conclude that cells from all cell lines have started to develop dendrites, an important step in MN differentiation and maturation.

$\beta$ TUBIII can be found in several structures of the nervous cells, including the cell body, dendrites, and axons. Therefore, its expression allows us to analyze the neuronal structure.

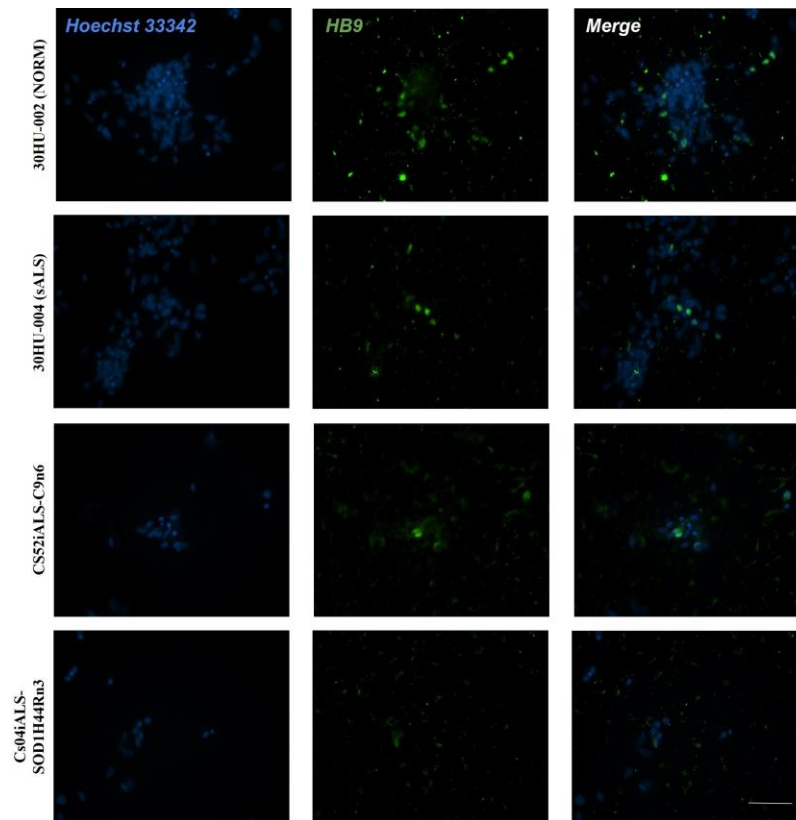


Figure 4.8: Immunocytochemical analysis of MNs at DIV30, stained for the marker HB9. The first row shows cells from the 30HU-002 (NORM) cell line, the second from the 30HU-004 (sALS) cell line, the third from the CS52iALS-C9n6 cell line, and the fourth from the Cs04iALS-SOD1H44Rn3 cell line. Scale bar = 50  $\mu$ m.

In Figure 4.10, it is possible to observe cells in the last stage of differentiation. MNs have further developed and matured, and it is possible to observe further elaboration of neurites and increased branching, reflecting the development of a more complex neuronal network.

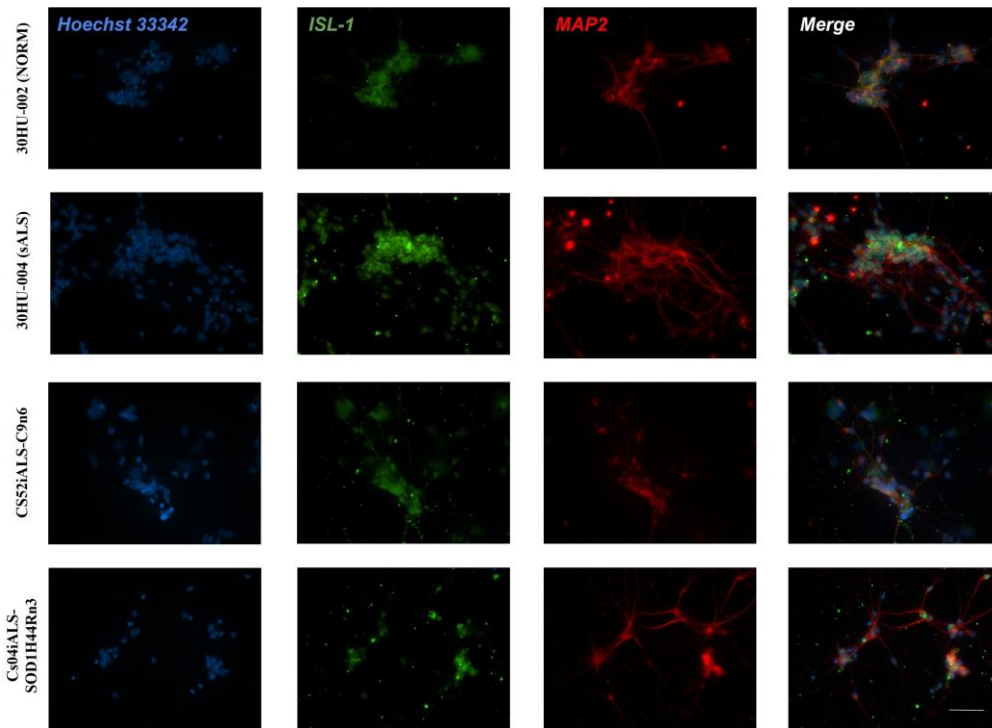


Figure 4.9: Immunocytochemical analysis of MNs at DIV30, stained for the markers ISL-1 and MAP2. The first row shows cells from the 30HU-002 (NORM) cell line, the second from the 30HU-004 (sALS) cell line, the third from the CS52iALS-C9n6 cell line, and the fourth from the Cs04iALS-SOD1H44Rn3 cell line. Scale bar = 50  $\mu$ m.

This phenomenon signifies the establishment of a more intricate neuronal network within the culture. The heightened complexity observed in these cells underscores the successful progression of motor neurons towards maturity and functional integration within neural circuits.

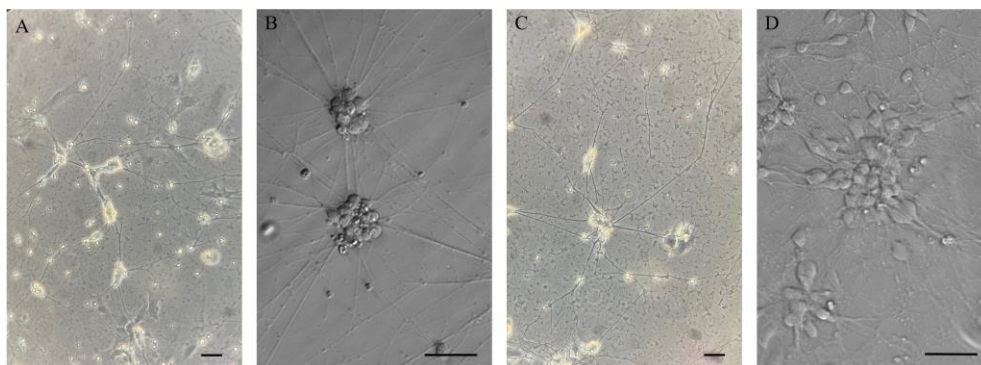


Figure 4.10: Bright Field (BF) images of iPSC colonies from four different cell lines in Medium D culture: (A) 30HU-002 (NORM), (B) 30HU-004 (sALS), (C) CS52iALS-C9n6, and (D) Cs04iALS-SOD1H44Rn3, respectively. Scale bar = 50  $\mu$ m

As a final analysis, at DIV40, the presence of the enzyme Choline Acetyltransferase (ChAT) was assessed. ChAT is the most specific marker for cholinergic neurons. This enzyme is responsible for the synthesis of *acetylcholine* (ACh), a neurotransmitter essential for cognitive and neuromuscular functions. In this analysis,  $\beta$ TUBIII was also immunostained to highlight the MN cytoskeleton. The primary and secondary antibodies used in this analysis are listed in Table A.2 (Appendix).

Since the expression levels of  $\beta$ TUBIII were similar at DIV30 and DIV40, only images from DIV40 are presented.

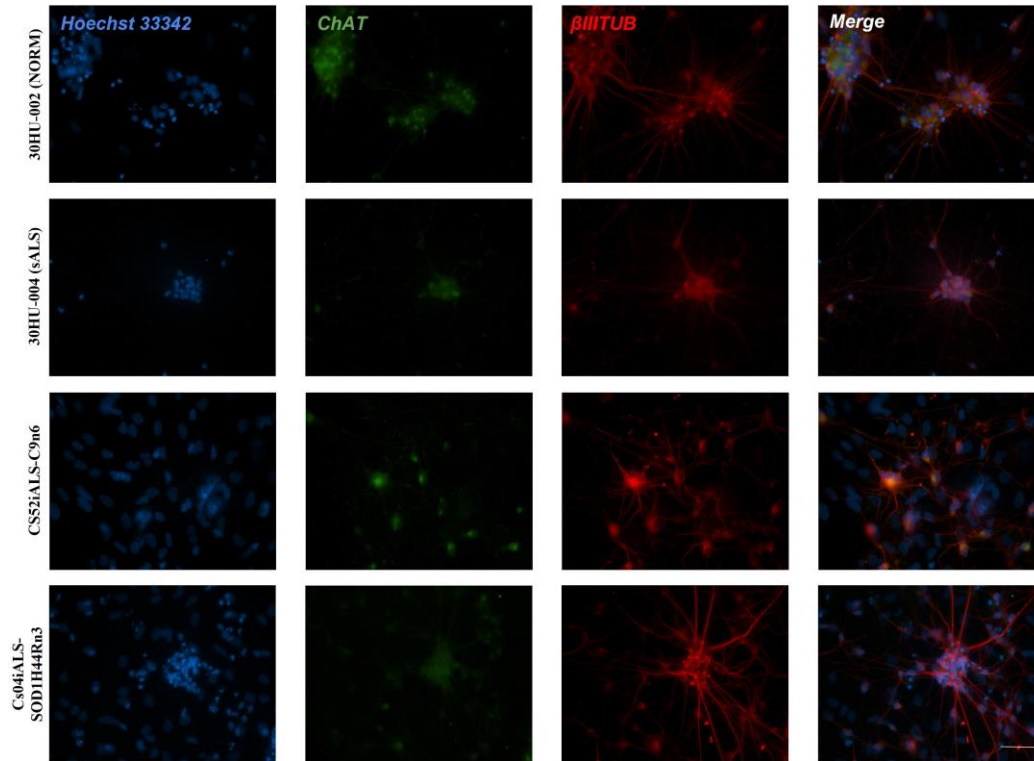


Figure 4.11: Immunocytochemical analysis of MNs at DIV40, stained for the markers ChAT and  $\beta$ TUBIII. The first row shows cells from the 30HU-002 (NORM) cell line, the second from the 30HU-004 (sALS) cell line, the third from the CS52iALS-C9n6 cell line, and the fourth from the Cs04iALS-SOD1H44Rn3 cell line. Scale bar = 50  $\mu$ m.

Observing Figure 4.11, it is possible to conclude that both markers are expressed in the cells, signifying the successful conclusion of the differentiation process and neuronal maturation.

Considering the immunopositivity of cells from all cell lines for all analyzed markers, it is possible to conclude that the inclusion of extrinsic signals in the culture medium promotes the differentiation of iPSC colonies, leading to the generation of mature MNs within these colonies.

## 4.2 Evaluation of the Differentiation Efficiency of iPSC-derived Motor Neurons

At the end of the differentiation process, a quantitative analysis to determine the procedure's efficiency was conducted. This analysis involved assessing the percentage of MNs obtained when compared to the total number of cells in culture.

In order to do this, cell immunostaining was conducted at DIV30. The cells were incubated with a primary antibody targeting  $\beta$ TUBIII. After this, the cells were treated with a fluorescence-conjugated secondary antibody, allowing for the visualization of the MN cytoskeleton. The staining of total nuclei was performed using *Hoechst* dye No. 33342. This enabled the visualization and quantification of the entire cell population in the culture.

Images were captured using a 20X objective lens of a digital camera mounted on a fluorescence microscope. Subsequently, images were processed using the ImageJ software. For each coverslip, cell counting was performed in fifteen distinct fields, with at least two coverslips analyzed for each condition. To calculate the differentiation percentage, the number of  $\beta$ TUBIII MNs was compared to the total number of cells present in the analyzed fields.

Table 4.1: Differentiation Efficiency of iPSCs into MNs.

Cell Line	Differentiation Efficiency (%)
30HU-002 (NORM)	88.94 ± 1.04
30HU-004 (sALS)	92.59 ± 1.12
CS52iALS-C9n6	93.60 ± 0.49
Cs04iALS-SOD1H44Rn3	70.61 ± 1.58

The data (mean ± S.E.M.) are shown as a percentage of the total number of cell nuclei present.

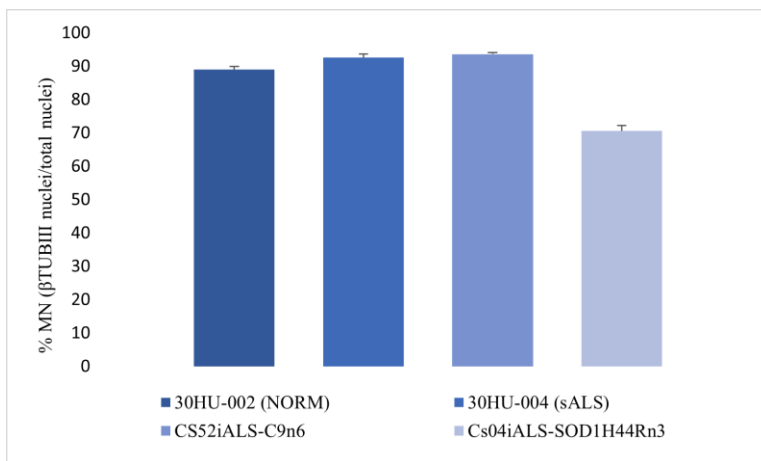


Figure 4.12: Differentiation Efficiency of iPSCs into MNs across four different cell lines: 30HU-002 (NORM), 30HU-004 (sALS), CS52iALS-C9n6, and Cs04iALS-SOD1H44Rn3, respectively.

The differentiation efficiency of iPSCs into MNs was evaluated in four different cell lines, as listed in Table 4.1 and shown in Figure 4.12. The majority of the lines showed a consistently high differentiation efficiency, especially the CS52iALS-C9n6 and 30HU-004 (sALS) cell lines. However, the Cs04iALS-SOD1H44Rn3 cell line exhibited a slight reduction in differentiation efficiency, suggesting that the process might be negatively impacted by the *SOD1* mutation. As mentioned in Section 2.4.3, this mutation can cause abnormal protein folding, which can result in protein aggregation and oxidative stress. These events may affect normal cellular homeostasis and the iPSCs' ability to differentiate into MNs. As a result, cells may respond less effectively to external differentiation signals, leading to a lower efficiency rate. Additionally, the mechanisms underlying the *SOD1* mutation can result in early apoptosis and reduced cell viability during differentiation, further affecting efficiency.

The 30HU-002 (NORM) cell line exhibited a high differentiation efficiency, which was similar to that observed in both the 30HU-004 (sALS) and the CS52iALS-C9n6 cell lines.

The fact that most ALS-specific cell lines demonstrated high differentiation efficiencies suggests that not all ALS-related mutations impact MN differentiation in the same way. These results indicate that the *SOD1* mutation affects differentiation pathways more seriously than the other ALS-related mutations.

Table 4.2: Statistical Analysis of Differentiation Efficiency of iPSC-derived MNs.

Cell Line Comparison	p-value	Significance
30HU-002 (NORM) vs 30HU-004 (sALS)	p <0.05	Statistically significant
30HU-002 (NORM) vs CS52iALS-C9n6	p <0.01	Statistically significant
30HU-002 (NORM) vs Cs04iALS-SOD1H44Rn3	p <0.0001	Statistically significant

In Table 11, it is possible to observe the results of the statistical analysis of the differentiation efficiency between the 30HU-002 (NORM) and the ALS-related cell lines. In this way, a p-value of <0.05 was observed between the 30HU-002 (NORM) and the 30HU-004 (sALS) cell lines, showing a slight increase in the 30HU-004 (sALS) line's differentiation efficiency, which indicates that the differentiation process is moderately affected by this mutation.

In the second comparison, between the 30HU-002 (NORM) and the CS52iALS-C9n6 cell lines, it was observed a p-value of <0.01. This indicates a more pronounced statistical difference, with the CS52iALS-C9n6 cell line exhibiting a more substantial increase in differentiation efficiency. Therefore, it seems that this mutation affects the differentiation process more significantly.

In the final comparison, between the 30HU-002 (NORM) and the Cs04iALS-SOD1H44Rn3 cell lines, a p-value of <0.0001 was obtained, which indicates a significant reduction in differentiation efficiency in the Cs04iALS-SOD1H44Rn3 cell line. This implies that this mutation is the one that impacts the differentiation process the most, possibly as a result of extensive cellular stress and dysfunction linked to this mutation.

### 4.3 Phenotypic Characterization of MNs Derived from iPSC: Neurite Length Evaluation

Once the differentiation efficiency was conducted, a morphological characterization was performed, consisting of the measurement of neurite length.

In order to do this, cells were immunostained at DIV30. The cells were labeled with primary and secondary antibodies targeting  $\beta$ TUBIII to allow visualization of the cell cytoskeleton, including the neuritic processes. Images were captured using a 20X objective lens of a digital camera mounted on a fluorescence microscope. Fifteen different fields were acquired for each coverslip, with at least two coverslips analyzed for each condition. After this, the average neurite length was assessed using the ImageJ software (NeuronJ plugin).

The data (mean  $\pm$  S.E.M.) are shown as absolute values of neurite length.

Table 4.3 and Figure 4.13 show the average neurite length of iPSC-derived MNs from four different cell lines.

According to these, the Cs04iALS-SOD1H44Rn3 cell line has the longest average neurite length, which

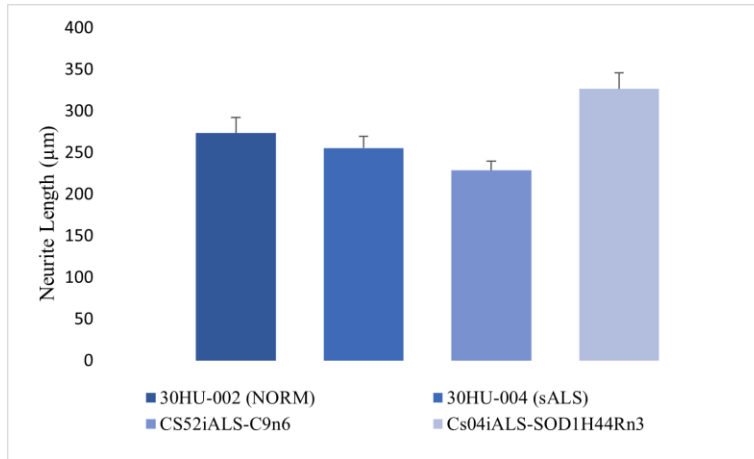


Figure 4.13: Average Neurite Length of MNs derived from four different cell lines: 30HU-002 (NORM), 30HU-004 (sALS), CS52iALS-C9n6, and Cs04iALS-SOD1H44Rn3, respectively.

Table 4.3: Average Neurite Length of iPSC-derived MNs.

Cell Line	Length (µm)
30HU-002 (NORM)	273.56 ± 18.54
30HU-004 (sALS)	255.49 ± 14.16
CS52iALS-C9n6	228.77 ± 10.70
Cs04iALS-SOD1H44Rn3	326.50 ± 19.56

is unexpected considering that it has the lowest differentiation efficiency. This could have two possible explanations. In the first place, despite the lower efficiency rate, there might have been higher neurite outgrowth in the MNs that did differentiate. In the second place, this could also mean that there are compensatory mechanisms or specific features of the *SOD1* mutation that affect neurite extension.

Additionally, the relatively long neurite length of the 30HU-002 (NORM) cell line is within expected limits for normal iPSC-derived MNs.

On the other hand, the 30HU-004 (sALS) and the CS52iALS-C9n6 cell lines exhibit shorter neurite lengths when compared to the 30HU-002 (NORM) cells. This indicates that the ALS-related mutations might affect neurite outgrowth, consistent with the disease's known neurodegenerative characteristics, often resulting in abnormal axonal growth and maintenance.

Table 4.4: Statistical Analysis of Neurite Length of iPSC-derived MNs.

Cell Line Comparison	p-value	Significance
30HU-002 (NORM) vs 30HU-004 (sALS)	No difference	Not statistically significant
30HU-002 (NORM) vs CS52iALS-C9n6	$p < 0.05$	Statistically significant
30HU-002 (NORM) vs Cs04iALS-SOD1H44Rn3	No difference	Not statistically significant

It is possible to observe in Table 13 the results of the statistical analysis of the neurite length between the 30HU-002 (NORM) and the ALS-related cell lines. The comparison between the 30HU-002 (NORM) and the 30HU-004 (sALS) cell lines revealed no statistically significant difference, suggesting that the neurite

length of the 30HU-004 (sALS) MNs that do differentiate is similar to the ones from the 30HU-002 (NORM) cell line.

On the other hand, the comparison between the 30HU-002 (NORM) and the CS52iALS-C9n6 cell lines shows a statistically significant difference, with a p-value of <0.05. This indicates that this mutation affects neurite outgrowth, resulting in shorter neurites of the MNs derived from the CS52iALS-C9n6 cell line.

Finally, the comparison between the 30HU-002 (NORM) and the Cs04iALS-SOD1H44Rn3 cell lines exhibits no statistically significant difference. This result suggests that this mutation may mainly affect differentiation efficiency rather than neurite extension in MNs.

#### 4.4 Analysis of ChAT expression levels

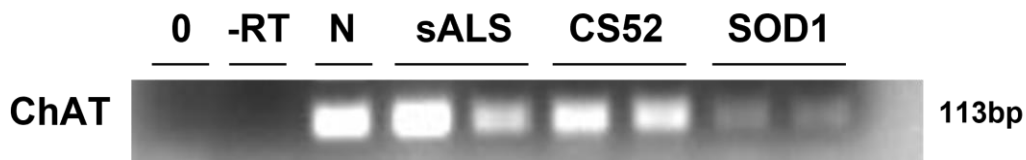


Figure 4.14: ChAT expression levels in four different cell lines: 30HU-002 (NORM, N), 30HU-004 (sALS), CS52iALS-C9n6 (CS52), and Cs04iALS-SOD1H44Rn3 (SOD1), respectively. The first two bands correspond to the control sample (labeled as 0) and the sample without reverse transcriptase (labeled as -RT), respectively.

The expression levels of ChAT were assessed in four iPSC-derived MN lines: 30HU-002 (NORM), 30HU-004 (sALS), CS52iALS-C9n6 (CS52), and Cs04iALS-SOD1H44Rn3 (SOD1). The resulting bands were observed in an electrophoresis gel image. It is expected that the ChAT transcript produces a band at 113 base pairs (bp) to confirm the successful transcription of the gene.

As shown in Figure 4.14, the first two bands represent controls: the first band (labeled as "0") is the control sample containing all the reagents required for the amplification except the cDNA. The absence of signal means that there was no contamination. The second band (labeled as "-RT") represents the sample without reverse transcriptase and shows no signal, guaranteeing the absence of false positives.

The 30HU-002 (NORM) cell line has a clear band, which means that the ChAT expression level is high.

The 30HU-004 (sALS) cell line shows a band of similar intensity to the NORM line, suggesting similar ChAT expression levels. However, one of the bands is lighter, which can have several explanations, such as cell population heterogeneity, epigenetic and transcriptional differences, or technical differences (including sample handling, RNA extraction, and loading of the gel).

The CS52iALS-C9n6 (CS52) cell line exhibits slightly fainter bands compared to the NORM and sALS bands, suggesting that there is a reduced expression level of ChAT in this cell line.

The Cs04iALS-SOD1H44Rn3 (SOD1) cell line has the faintest bands, indicating the lowest ChAT expression levels. This could be due to the intrinsic characteristics of the *SOD1* mutation, which can impair MN function and may restrict the ability to express ChAT efficiently.

## 5 Conclusion

In this study, a set of experimental phases were used to investigate the differentiation and maturation of iPSC-derived MNs. In order to do this, a range of cell lines were used, including lines from healthy individuals and from ALS patients with different mutations. In order to promote the differentiation process, the experimental protocol included the use of extrinsic signaling factors and optimized culture media. The evaluation of the differentiation process was performed through immunocytochemical techniques, with the assessment of stage-specific markers at several stages of differentiation. Furthermore, the morphological features of the resulting MNs were evaluated.

The results suggest that adding extrinsic differentiation signals to the culture medium stimulates the differentiation and subsequent maturation of iPSC-derived MNs. Nevertheless, lower immunopositivity for certain markers in the mutant *SOD1* cell line raises the possibility of line-specific problems, which could be caused by underlying genetic, epigenetic, or disease-related factors.

This study provides a comprehensive methodological framework for the *in vitro* generation of mature MNs and enhances our knowledge of iPSC-derived MNs. The results have important relevance for the study of neurodegenerative diseases, especially ALS. In addition, it might contribute to the creation of therapeutic approaches that specifically target motor neuron dysfunction.

In conclusion, important strategies could include the use of targeted extrinsic signals to further optimize differentiation protocols, the use of genetic and epigenetic profiling to identify mutations associated with differentiation, and the use of drug screening to determine which compounds improve differentiation or correct deficiencies in marker expression. These substances could have therapeutic potential in the treatment of ALS and other neurodegenerative diseases.

## Appendix

Table A.1: Information about the different cell lines used

Cell Line	ALS Type	Starting Cell Type	Reprogramming Method	Reprogramming Factors	Mutation	Gender	Age of onset (years)	Age at Tissue Sampling (years)	Disease Duration (months)	Manufacturer
30HU-002 (NORM)	-	Fibroblast	Episomal	-	-	Unknown	-	Unknown	-	iXCells Biotechnologies®
30HU-004	Sporadic	Fibroblast	Episomal	Unknown	Unknown	Female	Unknown	55	Unknown	iXCells Biotechnologies®
CS52iA LS-C9n6	Familial	Fibroblast	Episomal	Oct3/4, Sox2, Klf4, L-Myc, sph53, Lin28	C9orf72	Male	57	Unknown	48	Cedars-Sinai Biomanufacturing Center®
Cs04iA LS-SOD1H 44Rn3	Familial	Fibroblast	Episomal	Oct3/4, Sox2, Klf4, L-Myc, sph53, Lin28	SOD1	Female	Unknown	35	Unknown	Cedars-Sinai Biomanufacturing Center®

Table A.2: Immunocytochemistry on hiPSc in differentiation into MNs.

Time (Phase)	Permeabilization Solution	Blocking Solution	Primary Antibody	Secondary Antibody
For NEP cells	PBS1X + 0.25% Tx	PBS1X + 0.1% Tx + 5% NHS	#AF3369 - goat pol SOX1 1:20	#A11055 - DONKEY anti goat A488 1:200
For MNP cells	PBS1X + 0.25% Tx	PBS1X + 0.1% Tx + 5% NGS	#AB9610 - rabbit pol OLI2 1:100	#A11034 - GOAT anti rabbit A488 1:200
For mature MN cells	PBS1X + 0.25% Tx	PBS1X + 0.1% Tx + 5% NRS	#AB144P - goat pol CHAT 1:50	#A27012 - RABBIT anti goat A488 1:100
		PBS1X + 0.1% Tx + 5% NGS	#T8660 - mouse bTUB 1:500	#A11004 - GOAT anti mouse A568 1:200
		PBS1X + 0.1% Tx + 5% NGS	#815C.10 - mouse HB9 1:10 1:50	#A11001 - GOAT anti mouse A488 1:100
		PBS1X + 0.1% Tx + 5% NGS	#AB4326 - rabbit ISL-1 1:100 #M4403 - mouse MAP2 1:200	#A11034 - GOAT anti rabbit A488 1:200 #A11004 - GOAT anti mouse A568 1:200

## References

- [1] K. C. Flynn. The cytoskeleton and neurite initiation. *BioArchitecture*, 3(4):86–109, July 2013.
- [2] F. Akçimen, E. R. Lopez, J. E. Landers, A. Nath, A. Chiò, R. Chia, and B. J. Traynor. Amyotrophic lateral sclerosis: Translating genetic discoveries into therapies. *Nature Reviews Genetics*, 24(9):642–658, Apr 2023.
- [3] D. S. Younger and R. H. Brown. Amyotrophic lateral sclerosis. *Handbook of Clinical Neurology*, pages 203–229, 2023.
- [4] G. D. Hammer and S. J. McPhee. *Pathophysiology of disease: An introduction to clinical medicine*. McGraw-Hill Medical, 2018.
- [5] C. Shum, et al. Utilizing induced pluripotent stem cells (iPSCs) to understand the actions of estrogens in human neurons. *Hormones and Behavior*, 74:228–242, 2015.
- [6] E. O. Talbott, A. M. Malek, and D. Lacomis. The epidemiology of amyotrophic lateral sclerosis. *Neuroepidemiology*, pages 225–238, 2016.
- [7] L. P. Rowland and N. A. Shneider. Amyotrophic lateral sclerosis. *New England Journal of Medicine*, 344(22):1688–1700, May 2001.
- [8] M. X. Doss and A. Sachinidis. Current challenges of iPSC-based disease modeling and therapeutic implications. *Cells*, 8(5):403, 2019.
- [9] X. Wang. Stem cells in tissues, organoids, and cancers. *Cellular and Molecular Life Sciences*, 76(20):4043–4070, Jul 2019.
- [10] Z.-W. Du, et al. Generation and expansion of highly pure motor neuron progenitors from human pluripotent stem cells. *Nature Communications*, 6(1):7626, 2015.
- [11] M. P. McKinley and V. D. O’Loughlin. *Human anatomy*. McGraw-Hill, 2014.
- [12] C. L. VanPutte, J. L. Regan, and A. F. Russo. *Seeley’s Essentials of Anatomy and Physiology: 9th Edition*. McGraw-Hill Education, 2016.
- [13] N. Stifani. Motor neurons and the generation of spinal motor neuron diversity. *Frontiers in Cellular Neuroscience*, 8, Oct 2014.
- [14] L. C. Zayia. Neuroanatomy, motor neuron. Jul 2023.
- [15] C. B. Ivanhoe and T. A. Reistetter. Spasticity. *American Journal of Physical Medicine & Rehabilitation*, 83(Supplement), Oct 2004.

- [16] M. E. Héroux. Tap, tap, who's there? It's localized muscle activity elicited by the human stretch reflex. *The Journal of Physiology*, 595(14):4575–4575, Jun 2017.
- [17] S. Tajbakhsh and R. Spörle. Somite development: Constructing the vertebrate body. *Cell*, 92(1):9–16, Jan 1998.
- [18] A. Chandrasekhar. Turning heads: Development of vertebrate branchiomotor neurons. *Developmental Dynamics*, 229(1):143–161, Nov 2003.
- [19] B. Rexed. A cytoarchitectonic atlas of the spinal cord in the cat. *Journal of Comparative Neurology*, 100(2):297–379, Apr 1954.
- [20] J. C. Eccles, R. M. Eccles, A. Iggo, and A. Lundberg. Electrophysiological studies on gamma motoneurons. *Acta Physiologica Scandinavica*, 50(1):32–40, Sep 1960.
- [21] M. de Carvalho and M. Swash. Lower motor neuron dysfunction in ALS. *Clinical Neurophysiology*, 127(7):2670–2681, Jul 2016.
- [22] P. Bessou, F. Emonet-Dénand, and Y. Laporte. Motor fibres innervating extrafusal and intrafusal muscle fibres in the cat. *The Journal of Physiology*, 180(3):649–672, Oct 1965.
- [23] S. K. Gollapudi, J. J. Michael, and M. Chandra. Striated muscle dynamics. *Reference Module in Biomedical Sciences*, 2014.
- [24] R. D. Fields, A. Araque, H. Johansen-Berg, S.-S. Lim, G. Lynch, K.-A. Nave, M. Nedergaard, R. Perez, T. Sejnowski, and H. Wake. Glial biology in learning and cognition. *The Neuroscientist*, 20(5):426–431, Oct 2013.
- [25] K. R. Jessen and R. Mirsky. Glial cells in the enteric nervous system contain glial fibrillary acidic protein. *Nature*, 286(5774):736–737, Aug 1980.
- [26] H. Wolosker, E. Dumin, L. Balan, and V. N. Foltyn. d-amino acids in the brain: d-serine in neurotransmission and neurodegeneration. *The FEBS Journal*, 275(14):3514–3526, Jul 2008.
- [27] J. M. Rabey and F. Hefti. Neuromelanin synthesis in rat and human substantia nigra. *Journal of Neural Transmission - Parkinson's Disease and Dementia Section*, 2(1):1–14, Mar 1990.
- [28] J. Klingman. Functional recovery. *Archives of Neurology*, 45(6):645, Jun 1988.
- [29] M. Neumann, D. M. Sampathu, L. K. Kwong, A. C. Truax, M. C. Micsenyi, T. T. Chou, J. Bruce, T. Schuck, M. Grossman, C. M. Clark, and et al. Ubiquitinated TDP-43 in frontotemporal lobar degeneration and amyotrophic lateral sclerosis. *Science*, 314(5796):130–133, Oct 2006.
- [30] M. Yoshida. Neuropathology of amyotrophic lateral sclerosis. *PubMed*, 71(11):1152–1168, Nov 2019.

- [31] H.-X. Deng, W. Chen, S.-T. Hong, K. M. Boycott, G. H. Gorrie, N. Siddique, Y. Yang, F. Fecto, Y. Shi, H. Zhai, and et al. Mutations in UBQLN2 cause dominant X-linked juvenile and adult-onset ALS and ALS/dementia. *Nature*, 477(7363):211–215, Aug 2011.
- [32] D. S. Younger and J. Qian. Progressive muscular atrophy: A patient with confirmatory post-mortem findings. *Muscle & Nerve*, 51(4):621–623, Feb 2015.
- [33] D. S. Younger. Primary lateral sclerosis. *Archives of Neurology*, 45(12):1304, Dec 1988.
- [34] T. Siddique, D. A. Figlewicz, M. A. Pericak-Vance, J. L. Haines, G. Rouleau, A. J. Jeffers, P. Sapp, W.-Y. Hung, J. Bebout, D. McKenna-Yasek, and et al. Linkage of a gene causing familial amyotrophic lateral sclerosis to chromosome 21 and evidence of genetic-locus heterogeneity. *New England Journal of Medicine*, 324(20):1381–1384, May 1991.
- [35] J. Niwa, S. Yamada, S. Ishigaki, J. Sone, M. Takahashi, M. Katsuno, F. Tanaka, M. Doyu, and G. Sobue. Disulfide bond mediates aggregation, toxicity, and ubiquitylation of familial amyotrophic lateral sclerosis-linked mutant SOD1. *Journal of Biological Chemistry*, 282(38):28087–28095, Sep 2007.
- [36] C. A. Pardo, Z. Xu, D. R. Borchelt, D. L. Price, S. S. Sisodia, and D. W. Cleveland. Superoxide dismutase is an abundant component in cell bodies, dendrites, and axons of motor neurons and in a subset of other neurons. *Proceedings of the National Academy of Sciences*, 92(4):954–958, Feb 1995.
- [37] M. E. Cudkowicz, D. McKenna-Yasek, P. E. Sapp, W. Chin, B. Geller, D. L. Hayden, D. A. Schoenfeld, B. A. Hosler, H. R. Horvitz, and R. H. Brown. Epidemiology of mutations in superoxide dismutase in amyotrophic lateral sclerosis. *Annals of Neurology*, 41(2):210–221, Feb 1997.
- [38] Y. Hayashi, K. Homma, and H. Ichijo. SOD1 in neurotoxicity and its controversial roles in SOD1 mutation-negative ALS. *Advances in Biological Regulation*, 60:95–104, Jan 2016.
- [39] E. Kabashi, P. N. Valdmanis, P. Dion, D. Spiegelman, B. J. McConkey, C. Vande Velde, J.-P. Bouchard, L. Lacomblez, K. Pochigaeva, F. Salachas, and et al. TARDBP mutations in individuals with sporadic and familial amyotrophic lateral sclerosis. *Nature Genetics*, 40(5):572–574, Mar 2008.
- [40] J. Sreedharan, I. P. Blair, V. B. Tripathi, X. Hu, C. Vance, B. Rogelj, S. Ackerley, J. C. Durnall, K. L. Williams, E. Buratti, and et al. TDP-43 mutations in familial and sporadic amyotrophic lateral sclerosis. *Science*, 319(5870):1668–1672, Mar 2008.
- [41] L. M. Besser, M. A. Teylan, and P. T. Nelson. Limbic predominant age-related TDP-43 encephalopathy (LATE): Clinical and neuropathological associations. *Journal of Neuropathology & Experimental Neurology*, 79(3):305–313, Nov 2019.
- [42] M. R. Turner, O. Hardiman, M. Benatar, B. R. Brooks, A. Chio, M. de Carvalho, P. G. Ince, C. Lin, R. G. Miller, H. Mitsumoto, and et al. Controversies and priorities in amyotrophic lateral sclerosis. *The Lancet Neurology*, 12(3):310–322, Mar 2013.

- [43] T. R. Suk and M. W. Rousseaux. The role of TDP-43 mislocalization in amyotrophic lateral sclerosis. *Molecular Neurodegeneration*, 15(1), Aug 2020.
- [44] Q. Xia, G. Wang, H. Wang, Q. Hu, and Z. Ying. Folliculin, a tumor suppressor associated with Birt–Hogg–Dubé (BHD) syndrome, is a novel modifier of TDP-43 cytoplasmic translocation and aggregation. *Human Molecular Genetics*, 25(1):83–96, Oct 2015.
- [45] M. Polymenidou, C. Lagier-Tourenne, K. R. Hutt, S. C. Huelga, J. Moran, T. Y. Liang, S.-C. Ling, E. Sun, E. Wancewicz, C. Mazur, and et al. Long pre-mRNA depletion and RNA missplicing contribute to neuronal vulnerability from loss of TDP-43. *Nature Neuroscience*, 14(4):459–468, Feb 2011.
- [46] T. J. Kwiatkowski, D. A. Bosco, A. L. LeClerc, E. Tamrazian, C. R. Vanderburg, C. Russ, A. Davis, J. Gilchrist, E. J. Kasarskis, T. Munsat, and et al. Mutations in the FUS/TLS gene on chromosome 16 cause familial amyotrophic lateral sclerosis. *Science*, 323(5918):1205–1208, Feb 2009.
- [47] C. Vance, B. Rogelj, T. Hortobagyi, K. J. De Vos, A. L. Nishimura, J. Sreedharan, X. Hu, B. Smith, D. Ruddy, P. Wright, and et al. Mutations in FUS, an RNA processing protein, cause familial amyotrophic lateral sclerosis type 6. *Science*, 323(5918):1208–1211, Feb 2009.
- [48] A. E. Renton, A. Chio, and B. J. Traynor. State of play in amyotrophic lateral sclerosis genetics. *Nature Neuroscience*, 17(1):17–23, Dec 2013.
- [49] T. Nomura, S. Watanabe, K. Kaneko, K. Yamanaka, N. Nukina, and Y. Furukawa. Intranuclear aggregation of mutant FUS/TLS as a molecular pathomechanism of amyotrophic lateral sclerosis. *Journal of Biological Chemistry*, 289(2):1192–1202, Jan 2014.
- [50] G. Nicolas and J. A. Veltman. The role of de novo mutations in adult-onset neurodegenerative disorders. *Acta Neuropathologica*, 137(2):183–207, Nov 2018.
- [51] N. Suzuki, M. Aoki, H. Warita, M. Kato, H. Mizuno, N. Shimakura, T. Akiyama, H. Furuya, T. Hokonohara, A. Iwaki, and et al. FALS with FUS mutation in Japan, with early onset, rapid progress and basophilic inclusion. *Journal of Human Genetics*, 55(4):252–254, Mar 2010.
- [52] S. Lattante, G. A. Rouleau, and E. Kabashi. TARDBP and FUS mutations associated with amyotrophic lateral sclerosis: Summary and update. *Human Mutation*, 34(6):812–826, Apr 2013.
- [53] A. Hubers, W. Just, A. Rosenbohm, K. Muller, N. Marroquin, I. Goebel, J. Hogel, H. Thiele, J. Altmuller, P. Nurnberg, and et al. De novo FUS mutations are the most frequent genetic cause in early-onset German ALS patients. *Neurobiology of Aging*, 36(11), Nov 2015.
- [54] S. H. Kim, N. P. Shanware, M. J. Bowler, and R. S. Tibbetts. Amyotrophic lateral sclerosis-associated proteins TDP-43 and FUS/TLS function in a common biochemical complex to co-regulate HDAC6 mRNA. *Journal of Biological Chemistry*, 285(44):34097–34105, Oct 2010.

- [55] Y. Khalfallah, R. Kuta, C. Grasmuck, A. Prat, H. D. Durham, and C. Vande Velde. TDP-43 regulation of stress granule dynamics in neurodegenerative disease-relevant cell types. *Scientific Reports*, 8(1), May 2018.
- [56] D. A. Bosco, N. Lemay, H. K. Ko, H. Zhou, C. Burke, T. J. Kwiatkowski, P. Sapp, D. McKenna-Yasek, R. H. Brown, and L. J. Hayward. Mutant FUS proteins that cause amyotrophic lateral sclerosis incorporate into stress granules. *Human Molecular Genetics*, 19(21):4160–4175, Aug 2010.
- [57] E. Majounie, A. E. Renton, K. Mok, E. G. P. Dopper, A. Waite, S. Rollinson, A. Chio, G. Restagno, N. Nicolaou, J. Simon-Sanchez, and et al. Frequency of the C9orf72 hexanucleotide repeat expansion in patients with amyotrophic lateral sclerosis and frontotemporal dementia: A cross-sectional study. *The Lancet Neurology*, 11(4):323–330, Apr 2012.
- [58] A. E. Renton, E. Majounie, A. Waite, J. Simon-Sanchez, S. Rollinson, J. R. Gibbs, J. C. Schymick, H. Laaksovirta, J. C. van Swieten, L. Myllykangas, and et al. A hexanucleotide repeat expansion in C9orf72 is the cause of chromosome 9p21-linked ALS-FTD. *Neuron*, 72(2):257–268, Oct 2011.
- [59] E. L. van der Ende, J. L. Jackson, A. White, H. Seelaar, M. van Blitterswijk, and J. C. van Swieten. Unravelling the clinical spectrum and the role of repeat length in C9orf72 repeat expansions. *Journal of Neurology, Neurosurgery & Psychiatry*, 92(5):502–509, Jan 2021.
- [60] Z. Xu, M. Poidevin, X. Li, Y. Li, L. Shu, D. L. Nelson, H. Li, C. M. Hales, M. Gearing, T. S. Wingo, and et al. Expanded GGGGCC repeat RNA associated with amyotrophic lateral sclerosis and frontotemporal dementia causes neurodegeneration. *Proceedings of the National Academy of Sciences*, 110(19):7778–7783, Apr 2013.
- [61] Y. Shi, S. Lin, K. A. Staats, Y. Li, W.-H. Chang, S.-T. Hung, E. Hendricks, G. R. Linares, Y. Wang, E. Y. Son, and et al. Haploinsufficiency leads to neurodegeneration in C9orf72 ALS/FTD human induced motor neurons. *Nature Medicine*, 24(3):313–325, Feb 2018.
- [62] M. DeJesus-Hernandez, I. R. Mackenzie, B. F. Boeve, A. L. Boxer, M. Baker, N. J. Rutherford, A. M. Nicholson, N. A. Finch, H. Flynn, J. Adamson, and et al. Expanded GGGGCC hexanucleotide repeat in noncoding region of C9orf72 causes chromosome 9p-linked FTD and ALS. *Neuron*, 72(2):245–256, Oct 2011.
- [63] K. Reddy, B. Zamiri, S. Y. R. Stanley, R. B. MacGregor, and C. E. Pearson. The disease-associated r(GGGGCC) repeat from the C9orf72 gene forms tract length-dependent uni- and multimolecular RNA G-quadruplex structures. *Journal of Biological Chemistry*, 288(14):9860–9866, Apr 2013.
- [64] A. Chio, G. Borghero, G. Restagno, G. Mora, C. Drepper, B. J. Traynor, M. Sendtner, M. Brunetti, I. Ossola, A. Calvo, and et al. Clinical characteristics of patients with familial amyotrophic lateral sclerosis carrying the pathogenic GGGGCC hexanucleotide repeat expansion of C9orf72. *Brain*, 135(3):784–793, Feb 2012.
- [65] M. Ramalho-Santos and H. Willenbring. On the origin of the term “stem cell”. *Cell Stem Cell*, 1(1):35–38, Jun 2007.

- [66] S. He, D. Nakada, and S. J. Morrison. Mechanisms of stem cell self-renewal. *Annual Review of Cell and Developmental Biology*, 25(1):377–406, Nov 2009.
- [67] A. Bongso and M. Richards. History and perspective of stem cell research. *Best Practice & Research Clinical Obstetrics & Gynaecology*, 18(6):827–842, Dec 2004.
- [68] M. R. Alison, R. Poulson, S. Forbes, and N. A. Wright. An introduction to stem cells. *The Journal of Pathology*, 197(4):419–423, Jun 2002.
- [69] A. Casado-Díaz. Stem cells in regenerative medicine. *Journal of Clinical Medicine*, 11(18):5460, Sep 2022.
- [70] D. M. Choumerianou, H. Dimitriou, and M. Kalmanti. Stem cells: Promises versus limitations. *Tissue Engineering Part B: Reviews*, 14(1):53–60, Mar 2008.
- [71] A. Birbrair and P. S. Frenette. Niche heterogeneity in the bone marrow. *Annals of the New York Academy of Sciences*, 1370(1):82–96, 2016.
- [72] K. Takahashi and S. Yamanaka. Induction of pluripotent stem cells from mouse embryonic and adult fibroblast cultures by defined factors. *Cell*, 126(4):663–676, 2006.
- [73] D. S. Latchman. Transcription factors: An overview. *The International Journal of Biochemistry & Cell Biology*, 29(12):1305–1312, Dec 1997.
- [74] R. Zahumenska et al. Induced pluripotency: A powerful tool for in vitro modeling. *International Journal of Molecular Sciences*, 21(23):8910, 2020.
- [75] A. Ray et al. An overview on promising somatic cell sources utilized for the efficient generation of induced pluripotent stem cells. *Stem Cell Reviews and Reports*, 17(6):1954–1974, 2021.
- [76] L. A. Murray et al. Fibroblasts. In *Asthma and COPD*, pages 193–200, 2009.
- [77] Fibroblast cells. <https://fibroblast.org/>. Accessed 3 May 2024.
- [78] S. Raab et al. A comparative view on human somatic cell sources for iPSC generation. *Stem Cells International*, 2014:1–12, 2014.
- [79] J. Yu et al. Induced pluripotent stem cell lines derived from human somatic cells. *Science*, 318(5858):1917–1920, 2007.
- [80] G. J. Pan et al. Stem cell pluripotency and transcription factor Oct4. *Cell Research*, 12(5–6):321–329, Dec 2002.
- [81] G. Wu and H. R. Schöler. Role of Oct4 in the early embryo development. *Cell Regeneration*, 3(1):3–7, 2014.

- [82] G. Shi and Y. Jin. Role of Oct4 in maintaining and regaining stem cell pluripotency. *Stem Cell Research & Therapy*, 1(5):39, 2010.
- [83] S. Masui et al. Pluripotency governed by Sox2 via regulation of Oct3/4 expression in mouse embryonic stem cells. *Nature Cell Biology*, 9(6):625–635, 2007.
- [84] K. Liu et al. The multiple roles for Sox2 in stem cell maintenance and tumorigenesis. *Cellular Signalling*, 25(5):1264–1271, 2013.
- [85] C. V. Dang. Function of the c-Myc oncogenic transcription factor. *Experimental Cell Research*, 253(1):63–77, Nov 1999.
- [86] C. V. Dang. C-Myc target genes involved in cell growth, apoptosis, and metabolism. *Molecular and Cellular Biology*, 19(1):1–11, 1999.
- [87] J. Zhang et al. Lin28 regulates stem cell metabolism and conversion to primed pluripotency. *Cell Stem Cell*, 19(1):66–80, Jul 2016.
- [88] J. Tsalikas and J. Romer-Seibert. Lin28: Roles and regulation in development and beyond. *Development*, 142(14):2397–2404, Jul 2015.
- [89] N. Gawlik-Rzemieniewska and I. Bednarek. The role of Nanog transcriptional factor in the development of malignant phenotype of cancer cells. *Cancer Biology & Therapy*, 17(1):1–10, 2015.
- [90] J. Kaczynski et al. Sp1- and Kruppel-like transcription factors. *Genome Biology*, 4(2):206, 2003.
- [91] A. R. Black et al. Sp1 and Kruppel-like factor family of transcription factors in cell growth regulation and cancer. *Journal of Cellular Physiology*, 188(2):143–160, 2001.
- [92] M. O. Nandan and V. W. Yang. The role of Kruppel-like factors in the reprogramming of somatic cells to induced pluripotent stem cells. *PubMed*, 24(10):1343–1355, 2009.
- [93] N. Rawat and M. K. Singh. Induced pluripotent stem cell: A headway in reprogramming with promising approach in regenerative biology. *Veterinary World*, 10(6):640–649, Jun 2017.
- [94] K. Hu. All roads lead to induced pluripotent stem cells: The technologies of iPSC generation. *Stem Cells and Development*, 23(12):1285–1300, 2014.
- [95] N. Maherali and K. Hochedlinger. Guidelines and techniques for the generation of induced pluripotent stem cells. *Cell Stem Cell*, 3(6):595–605, Dec 2008.
- [96] T. M. Schlaeger et al. A comparison of non-integrating reprogramming methods. *Nature Biotechnology*, 33(1):58–63, 2015.
- [97] M. A. Amorós et al. Motor neuron-derived induced pluripotent stem cells as a drug screening platform for amyotrophic lateral sclerosis. *Frontiers in Cell and Developmental Biology*, 10:962881, 2022.

- [98] W. Zakrzewski et al. Stem cells: Past, present, and future. *Stem Cell Research & Therapy*, 10(1):1–22, 2019.
- [99] K. Takahashi et al. Induction of pluripotent stem cells from adult human fibroblasts by defined factors. *Cell*, 131(5):861–872, Nov 2007.
- [100] National Cancer Institute. Teratoma - nci dictionary of cancer terms, 2011. Accessed: 2024-05-29.
- [101] S. Sances et al. Modeling ALS using motor neurons derived from human induced pluripotent stem cells. *Nature Neuroscience*, 19(4):542–553, 2016.
- [102] C. Y. Chang et al. Induced pluripotent stem cells: A powerful neurodegenerative disease modeling tool for mechanism study and drug discovery. *Cell Transplantation*, 27(11):1588–1602, 2018.
- [103] Y. Maury et al. Combinatorial analysis of developmental cues efficiently converts human pluripotent stem cells into multiple neuronal subtypes. *Nature Biotechnology*, 33(1):89–96, 2014.
- [104] S. M. Chambers et al. Highly efficient neural conversion of human ES and iPS cells by dual inhibition of Smad signaling. *Nature Biotechnology*, 27(3):275–280, 2009.
- [105] C. Y. Chang et al. Induced pluripotent stem cell (iPSC)-based neurodegenerative disease models for phenotype recapitulation and drug screening. *Molecules (Basel, Switzerland)*, 25(8):2000, 2020.
- [106] A. M. Gois et al. In vitro and in vivo models of amyotrophic lateral sclerosis: An updated overview. *Brain Research Bulletin*, 159:32–43, Jun 2020.
- [107] P. Rivetti di Val Cervo et al. HiPSCs for predictive modeling of neurodegenerative diseases: Dreaming the possible. *Nature Reviews Neurology*, 17(6):381–392, 2021.
- [108] J. D. Miller et al. Human iPSC-based modeling of late-onset disease via progerin-induced aging. *Cell Stem Cell*, 13(6):691–705, 2013.
- [109] E. Inagaki et al. Accelerated neuronal aging in vitro ~melting watch~. *Frontiers in Aging Neuroscience*, 14, 2022.
- [110] S. S. C. Hung et al. Drug discovery using induced pluripotent stem cell models of neurodegenerative and ocular diseases. *Pharmacology & Therapeutics*, 177:32–43, 2017.
- [111] M. Redman et al. What is CRISPR/Cas9? *Archives of Disease in Childhood - Education & Practice Edition*, 101(4):213–215, Apr 2016.
- [112] M. W. Nicholson et al. Utility of iPSC-derived cells for disease modeling, drug development, and cell

therapy. *Cells*, 11(11):1853, 2022.

[113] A. J. Orqueda et al. iPSCs: A minireview from bench to bed, including organoids and the CRISPR system. *Stem Cells International*, 2016:1–9, 2016.

[114] D. Little et al. Using stem cell-derived neurons in drug screening for neurological diseases. *Neurobiology of Aging*, 78:130–141, 2019.

[115] Y. C. Wu et al. Blood–brain barrier and neurodegenerative diseases—modeling with iPSC-derived brain cells. *International Journal of Molecular Sciences*, 22(14):7710, 2021.

[116] B. Feng et al. Autophagy-mediated inflammatory cytokine secretion in sporadic ALS patient iPSC-derived astrocytes. *Oxidative Medicine and Cellular Longevity*, 2022:1–13, 2022.

[117] K. Imamura et al. The Src/c-Abl pathway is a potential therapeutic target in amyotrophic lateral sclerosis. *Science Translational Medicine*, 9(391):eaaf3962, 2017.

[118] E. G. Z. Centeno et al. 2D versus 3D human induced pluripotent stem cell-derived cultures for neurodegenerative disease modeling. *Molecular Neurodegeneration*, 13:1–14, 2018.

[119] A. E. Johns and N. J. Maragakis. Exploring motor neuron diseases using iPSC platforms. *Stem Cells*, 2022.